A new genus of rodent from Wallacea (Rodentia: Muridae: Murinae: Rattini), and its implication for biogeography and Indo-Pacific Rattini systematics

PIERRE-HENRI FABRE[1]*, MARIE PAGÈS[2,3], GUY G. MUSSER[4]†, YULI S. FITRIANA[5], JON FJELDSÅ[1], ANDY JENNINGS[6], KNUD A. JØNSSON[1], JONATHAN KENNEDY[1], JOHAN MICHAUX[3], GONO SEMIADI[5], NANANG SUPRIATNA[5] and KRISTOFER M. HELGEN[7]

[1]*Center for Macroecology, Evolution and Climate (CMEC, Department of Biology), Zoological Museum, University of Copenhagen, Universitetsparken 15, DK-2100 Copenhagen, Denmark*
[2]*Laboratoire de génétique des microorganismes, Université de Liège, 4000 Liège, Belgique*
[3]*INRA, UMR CBGP (INRA/IRD/Cirad/Montpellier SupAgro), Campus International de Baillarguet, CS 30016, 34988 Montferrier-sur-Lez Cedex, France*
[4]*Division of Vertebrate Zoology (Mammalogy), American Museum of Natural History, New York, NY 10024, USA*
[5]*Museum Zoologicum Bogoriense, Research Center For Biology, Indonesian Institute of Sciences (LIPI), Jl.Raya Jakarta-Bogor Km.46 Cibinong 16911 Indonesia*
[6]*Muséum National d'Histoire Naturelle, Département Systématique et Evolution CP 51, 57 Rue Cuvier, 75231 Paris, France*
[7]*National Museum of Natural History, Smithsonian. Institution, P.O. Box 37012, MRC 108, Washington, DC 20013-7012, USA*

We describe **Halmaheramys bokimekot** Fabre, Pagès, Musser, Fitriana, Semiadi & Helgen **gen. et sp. nov.**, a new genus and species of murine rodent from the North Moluccas, and study its phylogenetic placement using both molecular and morphological data. We generated a densely sampled mitochondrial and nuclear DNA data set that included most genera of Indo-Pacific Murinae, and used probabilistic methodologies to infer their phylogenetic relationships. To reconstruct their biogeographical history, we first dated the topology and then used a Lagrange analysis to infer ancestral geographic areas. Finally, we combined the ancestral area reconstructions with temporal information to compare patterns of murine colonization among Indo-Pacific archipelagos. We provide a new and comprehensive molecular phylogenetic reconstruction for Indo-Pacific Murinae, with a focus on the *Rattus* division. Using previous results and those presented in this study, we define a new Indo-Pacific group within the *Rattus* division, composed of *Bullimus*, *Bunomys*, *Paruromys*, *Halmaheramys*, *Sundamys*, and *Taeromys*. Our phylogenetic reconstructions revealed a relatively recent diversification from the Middle Miocene to Plio-Pleistocene associated with several major dispersal events. We identified two independent Indo-Pacific dispersal events from both western and eastern Indo-Pacific archipelagos to the isolated island of Halmahera, which led to the speciations of **H. bokimekot** gen. et sp. nov. and *Rattus morotaiensis* Kellogg, 1945. We propose that a Middle Miocene collision between the Halmahera and Sangihe arcs may have been responsible for the arrival of the ancestor of *Halmaheramys* to eastern Wallacea. **Halmaheramys bokimekot** gen. et sp. nov. is described in detail, and its systematics and biogeography are documented and illustrated.

© 2013 The Linnean Society of London, *Zoological Journal of the Linnean Society*, 2013, **169**, 408–447.
doi: 10.1111/zoj.12061

ADDITIONAL KEYWORDS: biodiversity – biogeography – Indo-Pacific – molecular systematics – morphology – Rattini – Wallacea.

*Corresponding author. E-mail: phfmourade@gmail.com
†Current address: 494 Wallace Drive, Charleston, SC 29412, USA.

INTRODUCTION

With more than 20 000 islands, ranging from small atolls to large tropical islands, the Indo-Pacific constitutes one of the most biotically important and geologically complex regions on the planet (Lohman *et al.*, 2011). Forty-five million years ago, the Australo-Papuan plate began to move northwards, culminating in a collision with the Asian and Pacific plates. This period of high tectonic activity (Hall, 2002, 2009) led to both the emergence and submergence of many islands (Hall, 1996; Hall, Cottam & Wilson, 2011). During the Plio-Pleistocene climate oscillations caused continuous sea level fluctuations, which periodically connected islands, or reduced the distances between them (Voris, 2000). This dynamic geological history has resulted in complex patterns of spatiotemporal dispersal and vicariance among lineages, and has generated a number of alternative scenarios of island colonization (Lohman *et al.*, 2011; Stelbrink *et al.*, 2012).

The most diverse terrestrial group of mammals within the Indo-Pacific region are rodents of the subfamily Murinae, represented by 368 extant species (Musser & Carleton, 2005; Aplin & Helgen, 2010). They mainly comprise three tribes (Lecompte *et al.*, 2008; Rowe *et al.*, 2008; Aplin & Helgen, 2010): the Phloeomyini (Philippine Old Endemics); the Rattini (rats and allies); and the Hydromyini. Both the Rattini and Hydromyini have colonized Australia, Melanesia, New Guinea, the Philippines, and Wallacea (Fig. 1). Throughout the Indo-Pacific, the complex distribution of the Murinae has been shaped by the history of dispersal, involving independent colonizations of different archipelagos (Jansa, Barker & Heaney, 2006; Rowe *et al.*, 2008). For example, in the Philippine murine assemblage (Heaney *et al.*, 1998, 2009; Rickart *et al.*, 2005) at least five independent colonizations from the Asian continent occurred during the Neogene (Jansa *et al.*, 2006). Two additional colonizations of Sahul regions (Australia and New Guinea) led to the respective diversification of
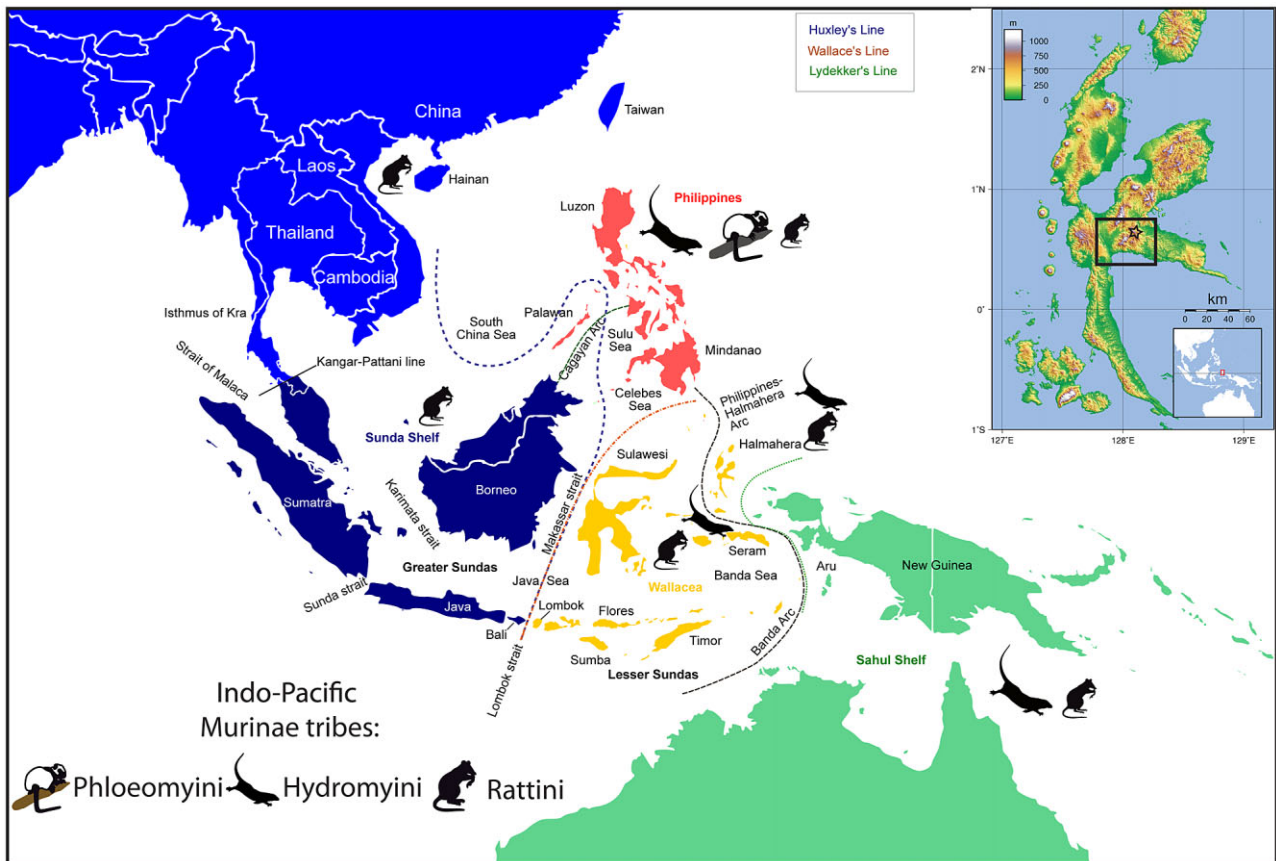
Figure 1. Map of the Indo-Pacific Archipelago indicating contemporary islands, straits, seas, arcs, and faunal lines (modified from Lohman *et al.*, 2011). Major islands are labelled; lineages of Murinae present on each island are also labelled; different countries in the Indo-Pacific are indicated by colours (see also Figs 2 and 3). Upper right: map of Halmahera Island, where a white star represents the trapping site of ***Halmaheramys bokimekot*** gen. et sp. nov. Maps were extracted and modified from Wikimapia (http://wikimapia.org).

the Australo-Papuan Hydromyini (Rowe *et al*., 2008; Bryant *et al*., 2011) and *Rattus* species (Taylor & Horner, 1973; Taylor, Calaby & Van Deusen, 1982; Robins *et al*., 2010; Rowe *et al*., 2011). Despite high murine species richness in Wallacea (more than 50 species; Musser, 1987), few molecular systematic analyses have addressed the biogeographic history of colonization in this region.

The Rattini is the most diverse tribe of murines in Wallacea (with more than 50 Sulawesian species, seven Lesser Sundaic species, and five Moluccan species). Systematic revisions continue to reveal overlooked diversity within the Rattini: 45 genera and 175 species are currently recognized, of which 66 are assigned to *Rattus*. The diversity of phenotypes in the Rattini (Ellerman, 1941, 1949; Misonne, 1969; Musser & Newcomb, 1983; Musser & Carleton, 2005), particularly within *Rattus* (Taylor *et al*., 1982; Musser & Holden, 1991; Musser & Carleton, 2005), represents a major challenge for Indo-Pacific rodent systematists (Medway & Yong, 1976; Musser, 1987). Most Rattini species exhibit morphological features reflecting mosaic convergences and plesiomorphies, generating considerable uncertainty in morphology-based classifications (Medway & Yong 1976; Musser & Newcomb, 1983; Musser & Holden, 1991). The systematic and taxonomic status of several genera within Rattini has been a topic of much debate, with many lineages traditionally regarded as part of *Rattus* now classified as separate genera (for reviews, see Musser & Newcomb 1983; Musser & Carleton, 2005). Based on recent molecular phylogenetic studies, the Rattini complex (Steppan *et al*., 2005; Rowe *et al*., 2008, 2011; Pagès *et al*., 2010; Balakirev *et al*., 2012; Esselstyn, Achmadi & Rowe, 2012) is considered to comprise 45 extant genera (for a tribal level classification of extant genera, see Aplin & Helgen, 2010; Table S1), split into five main groups: (1) the *Micromys* lineage; (2) the *Maxomys* and *Crunomys* divisions; (3) the *Dacnomys* division (*Chiromyscus*, *Dacnomys*, *Leopoldamys*, *Margaretamys*, *Niviventer*, *Saxatilomys*, and *Tonkinomys*); (4) the *Melasmothrix* division (*Melasmothrix*, *Paucidentomys*, *Sommeromys*, and *Tateomys*); and (5) the *Rattus* division (*Bandicota*, *Berylmys*, *Bullimus*, *Bunomys*, *Diplothrix*, *Paulamys*, *Kadarsonomys*, *Limnomys*, *Nesokia*, *Nesoromys*, *Palawanomys*, *Paruromys*, *Rattus*, *Srilankamys*, *Sundamys*, *Taeromys*, *Tarsomys*, and *Tryphomys*). The delimitation of species in some of these groups is particularly complex because of morphological homoplasy, heterogeneity in rates of molecular evolution, the potential for introgressive hybridization, and incomplete lineage sorting (Jansa *et al*., 2006; Balakirev & Rozhnov, 2010; Pagès *et al*., 2010, 2013; Buzan *et al*., 2011; Rowe *et al*., 2011).

Recent molecular studies have suggested that the centre of diversification for Rattini lies within South/Southeast Asia (Musser & Carleton, 2005; Rowe *et al*., 2008), from where they colonized various Indo-Pacific islands (Musser, 1981; Musser & Newcomb, 1983; Musser & Heaney, 1992). Specifically, members of the Rattini colonized the Philippines three times during the Late Miocene (*Bullimus*, *Limnomys* + *Tarsomys* + *Rattus everetti* group, *Crunomys* division; Jansa *et al*., 2006; Heaney *et al*., 2009), Sulawesi at least three times, also during the Miocene (*Bunomys* and *Rattus* group in *Rattus* division; *Maxomys* + *Crunomys* divisions; *Melasmothrix* division; Jansa *et al*., 2006; Rowe *et al*., 2008), and Sahul once, during the Pliocene (Australo-Papuan *Rattus*; Rowe *et al*., 2011).

Using the murine DNA sequences available, we aim to update the current understanding of the systematic relationships and colonization history of the Rattini within Wallacea, with a specific focus on the north Moluccas (Fig. 1). To achieve this, we sequenced four Rattini endemic to Sulawesi, one from Halmahera (*Rattus morotaiensis* Kellogg, 1945), and the newly discovered genus and species *Halmaheramys bokimekot* gen. et sp. nov., described here. Using mitochondrial and nuclear DNA sequences and dense taxon sampling, we infer a highly resolved molecular phylogeny. We subsequently use this phylogeny to compute ancestral area reconstructions of the Indo-Pacific Murinae in order to infer both the colonization history and patterns of speciation in this group. We aim to address the following questions: (1) what are the systematic affinities of Rattini lineages within the Indo-Pacific; (2) how many murine lineages are present in different archipelagos throughout the Indo-Pacific; and (3) what is the most likely scenario of dispersal events required to explain murine diversity patterns throughout the Wallacean archipelago, with a focus on Halmaheran endemics?

MATERIAL AND METHODS

TAXON AND GENE SAMPLING

Sequences were downloaded from GenBank/EMBL databases for one mitochondrial gene (cytochrome *b* apoenzyme: cyt *b*) and two nuclear genes (growth hormone receptor exon 10, *GHR*; interphotoreceptor retinoid binding protein exon 1, *IRPB*). We obtained sequences from 176 murine species, representing a total of 120 genera (following Musser & Carleton, 2005), from previous studies (Steppan *et al*., 2005; Jansa *et al*., 2006; Lecompte *et al*., 2008; Rowe *et al*., 2008; 2011; Heaney *et al*., 2009; Jansa, Giarla & Lim, 2009; Balete *et al*., 2012). Whenever possible, we selected sequences that were obtained from the same

voucher specimens, otherwise, we selected sequences giving congruent phylogenetic relationships among the genes, as inferred from phylogenetic inferences using RaXML (see following sections). Our analysis included the newly discovered Halmaheran murine *H. bokimekot* gen. et sp. nov. and the Halmaheran endemic *R. morotaiensis*. DNA sequences were also generated for the Sulawesi taxa *Bunomys andrewsi* Allen, 1911, *Bunomys chrysocomus* (Hoffmann, 1887), *Paruromys dominator* (Thomas, 1921), and *Taeromys celebensis* (Gray, 1867). We included the closest Rattini and Murinae out-groups, along with seven representatives of Deomyinae and Gerbillinae (Table S1) that are more distant out-groups (Michaux, Reyes & Catzeflis, 2001; Jansa & Weksler, 2004; Steppan, Adkins & Anderson, 2004; Jansa *et al.*, 2009). Four chimeras were built: three within the Gerbillinae (*Gerbillus*, *Gerbillurus*, and *Meriones*), and one within the Deomyinae (*Acomys*). To accomplish this, non-overlapping sequences (i.e. sequences available for different species of the same genus) were concatenated into the final multigene matrices. Sequences were aligned using MAFFT (Katoh & Toh, 2010) and checked with the ED editor of the MUST package (Philippe, 1993). From these individual alignments, we built four gene matrices: cyt *b* (191 taxa and 1140 sites; 5% of missing character states), *IRBP* (192 taxa and 1236 sites; 21% missing data), *GHR* (146 taxa and 937 sites; 11% missing data), and a nuclear plus mitochondrial supermatrix (204 taxa and 3313 sites; 23% missing data).

DNA AMPLIFICATION AND SEQUENCING

Ethanol-preserved samples were obtained from the mammalian tissue collections of the Museum Zoologicum Bogoriense (MZB; Cibinong, Indonesia), the Montpellier 2 University (CBGP; Montpellier, France), and from Operation Wallacea (Spilsby, UK). DNA was extracted from tissue with a DNEasy Tissue Kit (Qiagen), in accordance with the manufacturer's instructions. We sequenced the whole cyt *b* gene, and the *IRBP* and *GHR* fragments, according to protocols described elsewhere (Irwin, Kocher & Wilson, 1991; Poux & Douzery, 2004; Lecompte *et al.*, 2008; Pagès *et al.*, 2010). *IRBP* and *GHR* were obtained in two overlapping fragments. The genes were amplified and sequenced using the following primers: (1) cyt *b* (1242 bp), L14723 (5′-ACCAATGACATGAAAAATCAT CGTT-3′) and H15915 (5′-TCTCCATTTCTGGTTTAC AAGAC-3′); (2) IRBP1 (786 bp), I1-Rattus (5′-ATTGA GCAGGCTATGAAGAG-3′) and J2-Rattus (5′-TAGGG CTTGCTCYGCAGG-3′), and IRBP2 (893 bp), I2 (5′-ATCCCCTATGTCATCTCCTACYTG-3′) and J1 (5′-CGCAGGTCCATGATGAGGTGCTCCGTGTCCTG-3′); and (3) GHR1 (~690 bp), GHREXON10-fw (5′-GGRAA

RTTRGAGGAGGTGAACACMATCTT-3′) and GHR8-rev (5′-TTGGCATCTGACTCACAGAAGTAGG-3′), and GHR2 (~600 bp), GHR7-fw (5′-AAGCTGATCTCTTGT GCCTTGACCAGAA-3′) and GHR2-rev (5′-GATTTTG TTCAGTTGGTCTGTGCTCAC-3′). All amplifications were carried out in 25-µL reactions containing about 30 ng of extracted DNA, 100 µM of each dNTP, 0.2 µM of each primer, 1 unit of Taq polymerase (Qiagen), 2.5 µL of 10X buffer, 0.5 mM of extra $MgCl_2$. Cycling conditions were as follows: one activation step at 94 °C for 4 min, followed by 40 cycles of denaturation at 94 °C for 30 s, annealing at temperature depending on the primers (cyt *b*, 50 °C; IRBP1, 58 °C; IRBP2, 52 °C; GHR1, 58 °C; GHR2, 53 °C) for 30 s, elongation at 72 °C for 60–90 s, depending on the length of the target (1 min per kb), and a final extension at 72 °C for 10 min. PCR products were processed by the sequencing centre Genoscope (Evry, France) using an ABI 3730xl automatic capillary sequencer and the ABI BigDye Terminator v.3.1 sequencing kit. All sequences were analysed with CODONCODE ALIGNER software (CodonCode Corporation, Dedham, MA, USA).

PHYLOGENETIC ANALYSES ON THE INDIVIDUAL AND CONCATENATED GENES

Phylogenetic trees were reconstructed using both maximum likelihood (ML) and Bayesian inference for the single gene matrices and concatenated data sets independently. We used JMODELTEST 2.1.1 (Posada & Crandall, 1998; Posada, 2008) to determine the best-fitting ML model of DNA sequence evolution, as specified by the corrected Akaike's information criterion (AICc). Given the age of the subfamily Murinae (e.g. Steppan *et al.*, 2004; Lecompte *et al.*, 2008; Rowe *et al.*, 2008), the selected molecular markers could have been saturated and thereby could provide a spurious phylogeny (e.g. Xia *et al.*, 2003; Philippe *et al.*, 2011). We evaluated whether sequences were saturated with Xia's test (Xia *et al.*, 2003), implemented in the software program DAMBE (Xia & Xie, 2001; Xia & Lemey, 2009). This is an entropy-based index that estimates a substitution saturation index (Iss) and compares it with a critical substitution saturation index (Iss.c) via a randomization process, with 95% confidence intervals. Maximum likelihood parameters and topologies were estimated in PAUP* (Swofford, 2002) using a loop approach. To achieve this, the ML parameter values were first optimized on a neighbour-joining (NJ) topology obtained from ML distances, using the best-fitting substitution model. An ML heuristic search was subsequently applied with tree bisection and reconnection (TBR) branch swapping to select the optimal topology. The parameter values with the highest likelihood were then

re-estimated on this new topology. A subsequent heuristic tree search was then run using these new parameters. The loop procedure was performed until the stabilization of both topology and parameters was achieved. Support values for all nodes were estimated upon each matrix using ML in RAxML 7.0.4 (Stamatakis, 2006). This software can implement a partitioned analysis by applying: (1) a general time-reversible (GTR) model, with rate heterogeneity accounted for and a gamma (Γ) distribution (GTR + Γ); or (2) a GTR + CAT model (i.e. a GTR model with rate heterogeneity accounted for and a number of discrete rate categories), to each partition. For the partitioned data sets, we used the GTR + MIX option, which represents a combination of these two approaches. The GTR + MIX option assumes the faster GTR + CAT model for topological tree searches, and the GTR + Γ model when computing the likelihood value of each topology. All RAxML analyses used the default parameters, and comprised 10 000 tree pseudoreplicates. The node stability of the partitioned supermatrices was estimated using 10 000 nonparametric bootstrap replicates (Felsenstein, 1985). Bootstrap values were computed with RAxML using a GTR + MIX model.

To account for differences in the rates of DNA substitution among genes, we also applied a model-partitioned strategy for the analyses of the three supermatrices in a Bayesian framework. Bayesian analyses were performed in MrBayes 3.1.2 (Ronquist & Huelsenbeck, 2003), which allows different substitution models to be specified for each gene partition. The best-fitting models of substitution for these analyses were also identified using the AICc in JModelTest. All parameters, except the topology, were unlinked across partitions, and two independent runs with four Markov chain Monte Carlo (MCMC) algorithms were computed simultaneously, each with one cold and three heated chains. The MrBayes analyses were run for 35×10^7 generations, with trees sampled every 500 generations. In all cases, both the log-likelihood and model parameter values had reached stability by the end of the analysis. The majority-rule consensus tree was then computed after a burn-in of 3.5×10^5 generations.

To account for the potential differences in DNA substitution rates in the combined matrices, Bayesian analyses were performed under the CAT + G_4 mixture model (Lartillot & Philippe, 2004) using Phylobayes 3 (Lartillot, Lepage & Blanquart, 2009). For each supermatrix, two chains were run for 100 000 generations, and trees were sampled every 100 generations after the first 25 000 cycles. Convergence was achieved when the maximum difference of each bipartition frequency between the two chains was below 0.1.

MOLECULAR DATING

Divergence times were estimated from the combined mitochondrial + nuclear supermatrix to provide a temporal framework for Rattini evolution. A Bayesian relaxed molecular clock method was used to estimate divergence dates whilst accounting for changes in evolutionary rates through time, by allowing for independent models of sequence evolution for each gene partition. The best-fitting substitution models for each partition were selected according to the JModelTest results (Posada & Crandall, 1998; Posada, 2008). We used BEAST 1.7.4 (Drummond *et al*., 2002; Drummond & Rambaut, 2007) for phylogenetic analyses, assuming the Yule model of speciation and an uncorrelated log-normal distribution molecular clock (Ho, Kolokotronis & Allaby, 2007) as tree priors. Clock models were unlinked across gene partitions in order to account for missing data (Lemmon *et al*., 2009). We implemented the four clock models available in BEAST (strict, uncorrelated log-normal, uncorrelated exponential, and random local) to test the fit of different clock models to our molecular data set. Bayes factors were then calculated to determine the support for alternative states at each node of interest. Bayes factors (BFs) measure twice the difference between the log of the harmonic means (HMs) inferred by the clock models. We ran MCMC chains for 250 million generations, with trees sampled every 10 000 generations. We performed the analyses four times to check for the convergence of the model parameter estimates, and the program Tracer (Rambaut & Drummond, 2007) was used to assess algorithim convergence. We removed the first 15% of trees before the algorithm had reached stability as a burn-in. Trees from each of the four independent runs were combined into a maximum clade credibility tree with mean node heights using TreeAnnotator.

To calibrate the phylogeny, we selected six fossil constraints, as described from previous studies (Steppan *et al*., 2004; Jansa *et al*., 2006; Lecompte *et al*., 2008; Rowe *et al*., 2008, 2011). In order to take into account uncertainties in the phylogenetic position of these fossils, all constraints were set using hard minimum and soft upper boundaries, using a lognormal prior, as suggested by recent palaeontological studies (Benton & Donoghue, 2007; Benton, Donoghue & Asher, 2009; Parham *et al*., 2012). We used the following constraints:

1. The most recent common ancestor (MRCA) among the core Murinae was used to calibrate the divergence within this subfamily. Fossil evidence (Jacobs & Flynn, 2005) indicates that the acquisition of a major synapomorphy (full fusion of the lingual cusps with the medial and labial cusps)

within the core murine taxa occurred approximately 12.1 Mya (upper 95%, 10.01–22.9 Mya; Jacobs & Pilbeam, 1980; Jaeger, Tong & Denys, 1986; Jacobs *et al.*, 1990; Jacobs & Downs, 1994). This minimum boundary corresponds to the Middle Miocene split between *Antemus* and *Progonomys*. Because of the uncertainty of the sister taxa of the fossils used to calibrate this node (see Steppan *et al.*, 2004; Rowe *et al.*, 2008, 2011), we applied this constraint in two ways: the *Phloeomys/Batomys* split from the rest of the core Murinae; and the core Murinae divergence.

2. We used the stem Apodemurini fossils (11 Mya min) from the Early Vallesian (Late Miocene, 11.6–24.5 Mya; Martin Suarez & Mein 1998; Vangegeim, Lungu & Tesakov, 2006) to constrain the split between Apodemurini/Millardini (MRCA of *Apodemus/Tokudaia*) and Praomyini/Murini (MRCA of the *Mus/Praomys/Mastomys* clade; upper 95%, 8.91–21.8 Mya).

3. The MRCA of the *Apodemus mystacinus* and the *Sylvaemus* groups [affiliated with *Apodemus flavicollis* (Melchior, 1834) and *Apodemus sylvaticus* (Linnaeus, 1758), respectively] were constrained using the *Apodemus* fossil record (Aguilar & Michaux, 1996; Michaux *et al.*, 1997) from the Upper Miocene. We set a median prior age of 7 Myr (upper 95%, 5.96–12.37 Myr).

4. We used the first fossil record of *Mus* (*Mus auctor* Jacobs 1978; Jacobs *et al.*, 1990; Jacobs & Downs, 1994; Lundrigan, Jansa & Tucker, 2002) to represent the minimum divergence at 5.7 Mya (upper 95%, 4.66–11.07 Mya) between different *Mus* lineages [*Mus musculus* (Linnaeus, 1758)/*Mus pahari* (Thomas, 1916)/*Mus setulosus* (Peters, 1876); Jacobs & Downs, 1994].

5. We used the African crown Arvicanthini lineage from the late Miocene (median age 6 Myr; from the Tortonian; Winkler, 2002) and a soft maximum prior extending to the Serravalian (upper 95%, 3.91–16.81 Mya) as a constraint of the MRCA of Arvicanthini.

6. We set a minimum constraint for the MRCA of Hydromyini, using the first Australian fossil evidence dated at 3.4 Mya (upper 95%: 1.3–14.21 Mya; Tedford, Wells & Barghoorn, 1992; Aplin, 2006; Rowe *et al.*, 2008).

We performed analyses using (1) all fossil constraints implemented simultaneously (with both *Antemus/Progonomys* split constraints) and (2) with a cross-validation approach for the *Antemus/Progonomys* split constraints (by removing this constraint). We assessed convergence in the dating estimates using the full and sub-sampled data sets; the results were similar. For the 'excluded constraint' and the 'all constraints' approaches, the molecular and fossil estimated divergence dates were compared.

BIOGEOGRAPHICAL ANALYSIS

To study the biogeographical history of Indo-Pacific murines, we calculated ancestral area reconstructions using the phylogenies estimated as described above, in Lagrange (Ree *et al.*, 2005, Ree & Smith, 2008) This method implements the dispersal–extinction–cladogenesis (DEC) model to compute likelihood values for ancestral ranges, in addition to the timing and directionality of dispersal events. In this analysis ancestral areas are optimized onto the internal nodes, enabling ML estimation of the ancestral states (range inheritance scenarios) by modelling transitions between discrete states (biogeographical ranges) as a function of time. Because no extant species occupies more than three regions [excluding the human commensals *Rattus argentiventer* (Robinson & Kloss, 1916), *Rattus exulans* (Peale, 1848), *Rattus nitidus* (Hodgson, 1845), *Rattus norvegicus* (Berkenhout, 1769), *Rattus rattus* (Linnaeus, 1758), *Rattus tanezumi* (Temminck, 1844), *Rattus tiomanicus* (Miller, 1900)], the analysis was performed constraining the maximum number of areas occupied by the ancestral lineages to two ranges using the maxareas (= 2) option in Lagrange.

We assigned six geographic areas for the Lagrange analysis, as follows: Africa, South/Southeast Asia + Sundaland (Bali, Borneo, Java, and Sumatra), the Palaearctic, the Philippines, Sahul (Australia + New Guinea), and Wallacea (Lesser Sunda, Molucca, and Sulawesi). The resulting reconstructions are summarized by area; areas with cumulative probabilities of ancestral area greater than 50% are plotted along the dated topology.

MORPHOMETRIC MEASUREMENTS

In tandem with our molecular comparisons, we used classical external, cranial, and dental qualitative morphological characters to quantify similarities and differences among *Halmaheramys* gen. nov., *Bullimus*, *Bunomys*, *Paruromys*, *Sundamys*, and *Taeromys*. We examined museum skins and associated skulls from the following institutions: the American Museum of Natural History, New York (AMNH); Natural History Museum, London (BMNH); Museum of Vertebrate Zoology, Berkeley, California (MVZ); Museum Zoologicum Bogoriense, Cibinong, Java (MZB); Nationaal Natuurhistorisch Museum Naturalis, Leiden (RMNH), South Australian Museum, Adelaide (SAM); and National Museum of Natural History, Smithsonian Institution, Washington, D.C.

Table 1. Descriptive measurements for lengths of head and body (HB), tail (TL), hind foot (HF), and ear (E), in mm, and for weight in grams (WT), in ***Halmaheramys bokimekot* gen. et sp. nov.**, *Paruromys dominator*, and selected species of *Bunomys* and *Taeromys*

Species	HB	TL	HF	E	WT	TL/HB (%)
***Halmaheramys* gen. nov.**						
H. bokimekot gen. et sp. nov. ♀	153.2 ± 12.33 (143.2–167.0) 3	121.6 ± 1.55 (119.9–122.9) 3	28.1 ± 0.48 (27.5–28.4) 3	18.4 ± 1.12 (27.5–28.4) 3	89.3 ± 15.04 (72–99) 3	79
H. bokimekot gen. et sp. nov. ♂	149.0 ± 2.71 (145.9–151.1) 3	126.0 ± 9.02 (119.6–132.3) 3	29.6 ± 0.49 (29.2–30.1) 3	18.9 ± 0.94 (18.1–19.9) 3	89.7 ± 8.50 (81–98) 3	85
Bunomys						
B. chrysocomus	161.5 ± 8.23 (133–180) 147	137.4 ± 10.75 (90–165) 139	35.9 ± 1.25 (33–39) 147	23.3 ± 0.96 (21–26) 146	93.3 ± 15.09 (55–135) 147	85
B. andrewsi	177.4 ± 11.62 (157–195) 17	150.1 ± 9.92 (130–161) 15	40.5 ± 1.33 (38–42) 17	24.7 ± 1.00 (23–26) 17	154.6 ± 33.43 (98–222) 17	85
B. penitus	184.0 ± 10.45 (155–242) 82	162.5 ± 8.63 (138–185) 76	41.4 ± 1.30 (38–44) 82	26.1 ± 0.91 (23–28) 82	133.3 ± 15.42 (95–170) 76	88
Taeromys						
T. celebensis	224.0 ± 13.83 (201–249) 22	274.6 ± 16.64 (244–306) 22	50.1 ± 2.16 (47–56) 22	26.6 ± 0.73 (25–28) 22	252.7 ± 36.68 (190–345) 22	123
T. callitrichus	233.8 ± 8.17 (220–240) 5	253.2 ± 7.79 (240–260) 5	52.6 ± 1.14 (51–54) 5	27.2 ± 0.84 (26–28) 5	318.6 ± 26.88 (290–363) 5	108
T. hamatus	197.9 ± 12.03 (180–213) 10	192.0 ± 11.07 (177–205) 9	43.6 ± 1.43 (42–46) 10	24.7 ± 0.48 (24–25) 10	181.8 ± 24.50 (145–220) 10	97
Paruromys						
P. dominator	249.1 ± 11.62 (225–275) 63	284.3 ± 14.10 (256–316) 63	54.3 ± 1.64 (51–60) 63	29.1 ± 1.22 (27–32) 63	324.9 ± 48.92 (220–425) 63	114

Mean ± SD, observed range (in parentheses), and size of sample are provided. Mean values were used to compute tail length (TL)/head–body length (HB). Samples of *Bunomys*, *Taeromys*, and *Paruromys* contain males and females, and are from central Sulawesi. Data listed here and in Tables 3–5 and 8 for the Sulawesi genera are extracted from Musser (pers. comm.).

(USNM). Specimens of *Bunomys*, *Taeromys*, and *Paruromys* used in our comparisons are listed in Appendix. Specimens obtained during the Halmahera expedition (January–February and June–July, 2010) were prepared in the field by representatives of MZB. Rodents were captured and handled in the field following guidelines approved by the American Society of Mammalogists. Images of both the holotype and five paratype skulls of *Halmaheramys bokimekot* gen. et sp. nov. were scanned (using a µCT scanner) and photographed, with images stored at the Plateforme Microtomographie (University of Montpellier). Photographs were taken with a BK+ Imaging System from Visionary Digital (http://www.visionarydigital.com), equipped with a Canon EOS 7D camera. Single images were combined with HELICON FOCUS 5.0 to increase depth of field (http://www.heliconsoft.com; Helicon Soft Ltd). Measurements of head–body length (HB), tail length (TL), hind foot length (including claws) (HF), ear length from the notch (E), and weight in grams (WT) for *H. bokimekot* gen. et sp. nov. were recorded by the original collectors in the field and extracted from a field catalogue stored at MZB (Table 1). All external measurements were taken either with a digital ruler or with PESOLA scales (graduated to 1 g). For *H. bokimekot* gen. et sp. nov., *P. dominator*, six species of *Bunomys*, and seven species of *Taeromys*, 16 cranial and two dental measurements were taken using a dial caliper graduated to 0.01 mm, (measurements as described by Musser & Newcomb, 1983): occipitonasal length (ONL), greatest zygomatic breadth (ZB), least interorbital breadth (IB), length of the rostrum (LR), breadth of the rostrum (BR), breadth of the braincase (BBC), height of the braincase (HBC), breadth of the zygomatic plate (BZP), length of the diastema (LD), postpalatal length (PPL), length of bony palate (LBP), breadth of the bony plate at first molar (BBPM1), breadth of the mesopterygoid fossa (BMF); length of the incisive foramen (LIF), breadth of the incisive foramen (BIF), length of auditory bulla (LB), crown length of the maxillary molar row (CLM1–3), and breadth of first upper molar (BM1). Specimens consist of intact skulls of male and

female adults (ranging from young to old), with between two and 260 individuals per species from each locality (see Results). The number of *Halmaheramys* specimens is small (*n* = 6), and consists of adults only (males displayed descended testes and females displayed enlarged nipples). Measurements were analysed by calculating descriptive univariate statistics (mean, standard deviation, and observed range) and employing principal component procedures. Principal component analyses were computed using original cranial and dental measurements transformed to natural logarithms. Measurements were log-transformed to normalize the distribution of variation. Principal components were extracted from a correlation matrix: the loading values (correlations) of the variables are given as Pearson product–moment correlation coefficients of the extracted principal components. Probability levels denoting the significance of the correlations in both kinds of analyses are unadjusted. The statistical packages in SYSTAT 11 for WINDOWS (2005) were used for all analytical procedures.

A list of the museum specimens used as comparative material is given in Appendix.

RESULTS

PHYLOGENETIC ANALYSES

Using Xia's test, we did not find significant evidence of saturation for *GHR* and *IRBP*, even when codon positions were considered separately (all Iss < Iss.c with significant results). For the mitochondrial cyt *b*, the whole partition alone did not show significant evidence of saturation; however, considering the third position of the codon seperately, we found substantial saturation (Iss < Iss.c with no significant results) relative to positions 1 and 2. In order to reduce problems of saturation and among-site substitution pattern heterogeneity, mixture models like CAT have been developed (Lartillot & Philippe, 2004). We used the GTR + CAT model to take into account any bias in composition, saturation, and gene/codon partitions (for further details, see Lartillot & Philippe 2009; Douzery 2011). The site-heterogeneous CAT model allows us to analyse mitochondrial and nuclear concatenates of different genes (*IRBP*, *GHR*, and cyt *b*). Because the CAT model groups sites into a number of independent categories, defined a posteriori, it accounts for site-specific nucleotide preferences.
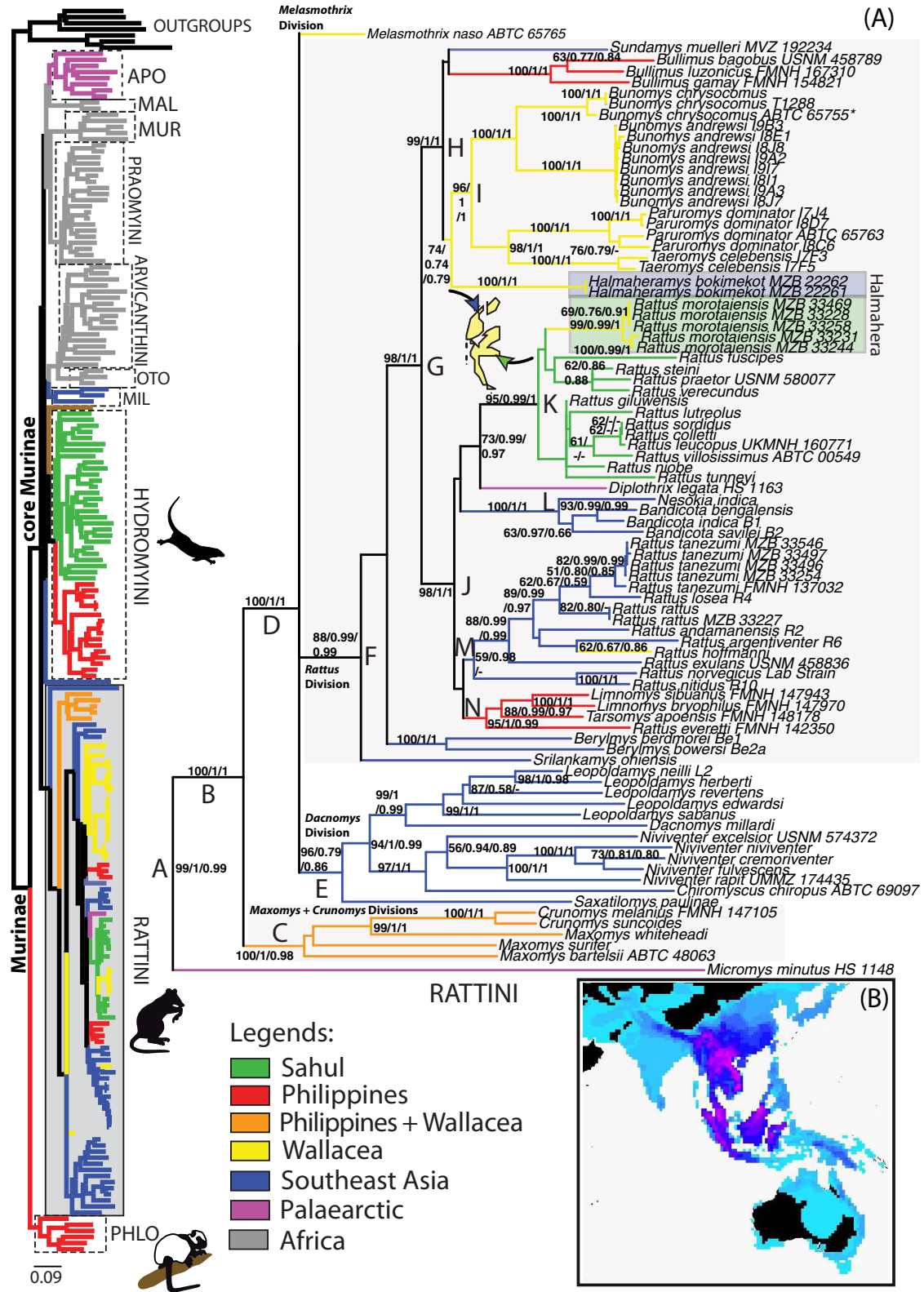
Phylogenetic analyses of the combined data set with single or multiple partitions yielded similar topological results, displayed in Figure 2. The Murinae (Fig. 2) were split into the Phloeomyini [ML bootstrap (BP = 100), MrBayes posterior probability (PP1 = 1), Phylobayes posterior probability (PP2 = 1)] and the

core Murine (BP = 100, PP1 = 1, PP2 = 1). We found support for three core murine clades: (1) the African Arvicanthini + Otomyini (BP = 100, PP1 = 1, PP2 = 1); (2) the Apodemurini + Malacomyini + Murini + Praomyini (BP = 85, PP1 = 0.99, PP2 = 0.99); and (3) a sister relationship between Millardini and the clade Arvicanthini + Otomyini (BP = 100, PP1 = 0.99, PP2 = 0.99). Relationships among these clades and among these different tribes, as well as some positions of members from the *Micromys* division (cf. *Chiropodomys* and *Vandeleuria*), are unresolved with our three-gene analysis. We further recovered nine monophyletic tribes with high support (cf. Apodemurini, Arvicanthini, Hydromyini, Millardini, Malacomyini, Murini, Otomyini, Praomyini, and Rattini), as found by the analyses of Lecompte *et al*. (2008) and Rowe *et al*. (2008) (BP > 95%, PP1 = 1, PP2 = 1).

Within the Rattini, we recovered a dichotomy between *Micromys minutus* (Pallas, 1771) and all other species (node A, BP = 99, PP1 = 1, PP2 = 0.99). A basal split was supported between the Southeast Asian *Maxomys* and the Philippine–Sulawesian *Crunomys* (node C; BP = 100, PP1 = 1, PP2 = 1). A clade containing the majority of the other Rattini species (node D; BP = 100, PP1 = 1, PP2 = 1) was then supported as sister to these taxa (node B). The *Maxomys* division is paraphyletic because of the inclusion of *Crunomys* (BP = 99, PP1 = 1, PP2 = 1). The remaining division includes three main lineages: the *Melasmothrix* lineage, the *Dacnomys* division (node E; BP = 96, PP1 = 0.79, PP2 = 0.86), and the *Rattus* division (node F; BP = 88, PP1 = 0.99, PP2 = 0.99). Within the *Dacnomys* division we recovered a basal split between *Saxatilomys* and a clade containing the other four genera (*Chiromyscus*, *Dacnomys*, *Leopoldamys*, and *Niviventer*). This last clade is split into two well-supported clades containing: (1) *Dacnomys + Leopoldamys* (BP = 99, PP1 = 1, PP2 = 0.99); and (2) *Chiromyscus + Niviventer* (BP = 97, PP1 = 1, PP2 = 1).

The *Rattus* division clade (node F) is split into four main lineages: (1) *Srilankamys ohiensis* (Phillips, 1929); (2) *Berylmys*; (3) a clade containing the Sulawesian *Bunomys*, *Paruromys*, and *Taeromys*, the Moluccan *Halmaheramys* gen. nov., the Philippine *Bullimus*, and the Sundaic *Sundamys* (node H; BP = 99, PP1 = 1, PP2 = 1); (4) a clade containing the Southeast Asian *Rattus* (node M; BP = 59, PP1 = 0.98, PP2 = –), the Philippine taxa *Limnomys*, *Tarsomys*, and *Rattus everetti* (Günther, 1879) (node N; BP = 95, PP1 = 1, PP2 = 0.99), the South/Southeast Asian *Nesokia + Bandicota* (node L; BP = 100, PP1 = 1, PP2 = 0.99), and a clade containing the Japanese *Diplothrix* and the Sahul *Rattus* (BP = 73, PP1 = 0.99, PP2 = 1). It is within this Sahul clade that *R. morotaiensis* belongs (node K; BP = 95, PP1 = 0.99, PP2 = 1). The endemic Moluccan *R. morotaiensis* is

(A)

(B)

RATTINI

Legends:
- Sahul (green)
- Philippines (red)
- Philippines + Wallacea (orange)
- Wallacea (yellow)
- Southeast Asia (blue)
- Palaearctic (magenta)
- Africa (grey)

closely related to *Rattus fuscipes* (Waterhouse, 1839) and a clade containing *Rattus steini* (Rümmler, 1935), *Rattus praetor* (Thomas, 1888), and *Rattus verecundus* (Thomas, 1904), but with low support.

Node H displays a polytomy among *Halmaheramys*, *Sundamys*, and a Sulawesian clade (node I, BP = 96, PP1 = 1, PP2 = 1). Within this Sulawesian clade, we recovered *Paruromys* and *Taeromys* as a monophyletic group (BP = 98, PP1 = 1, PP2 = 1), with *Bunomys* (node I).

MOLECULAR DATING AND BIOGEOGRAPHY

Comparison between a strict and a relaxed molecular clock provided a positive value, which meant that the strict molecular clock was rejected in our concatenated data set. The uncorrelated log-normal clock model returned the highest marginal log-likelihood [$\ln(L)_{\text{uncorrelated log-normal}} = -93759.1$ compared with $\ln(L)_{\text{strict}} = -93931.7$, $\ln(L)_{\text{uncorrelated exponential}} = -93759.4$, $\ln(L)_{\text{random local clock models}} = -93841.2$] and the highest BF, and was thus selected for our final analyses. Based on the relaxed molecular clock Bayesian analysis, a time scale for the evolution of the Murinae is depicted in Table 2.

The results of the Bayes–Lagrange analyses are shown in Figures 3 and 4. The origin of the Murinae and core Murinae appears to have been in the Southeast Asia/Philippine region, with the ancestor of Rattini and Hydromyini originating in Southeast Asia (Fig. 3) in the Late Miocene. Several major waves of dispersal and colonization are inferred by our phylogenetic and Lagrange results for the Indo-Pacific region (Fig. 4). An early diversification in the Philippines is indicated for the Phloeomyini tribe, with an inferred origin both in Southeast Asia and in the Philippines [MRCA, 11.6 Mya (10.2–13.0 Mya); Philippine diversification, 8.41 Mya (6.7–10.2 Mya)]. The Hydromyini tribe underwent an expansion in both Sahul [MRCA, 8.5 Mya (7.4–9.6 Mya); Sahul diversification, 6.8 Mya (5.9–7.7 Mya)] and the Philippines [MRCA, 8.5 Mya (7.4–9.6 Mya); Philippine diversification, 5.4 Mya (4.5–6.3 Mya)]. Within Rattini, we inferred at least three colonizations of the Philippines, at least five colonizations of Wallacea (Sulawesi and Moluccas), and one colonization of Sahul. There were two Late Miocene/Early Pliocene colonizations, with the diversification of the *Melasmothrix* division in Sulawesi [MRCA, 5.89 Mya (5.0–6.8 Mya)], and the diversification of the *Maxomys* and *Crunomys* division in both the Philippines and Sulawesi [MRCA, 6.97 Mya (6.0–8.0 Mya); Philippines/Sulawesi diversification, 4.8 Mya (3.76–5.9 Mya)]. Several Plio-Pleistocene colonizations of Indo-Pacific archipelagos from a Southeast Asian Rattini ancestor are also inferred from our analysis (Fig. 4). Two Philippine diversifications involve *Bullimus* [MRCA, 3.1 Mya (2.5–3.6 Mya); Philippines diversification, 1.1 Mya (0.8–1.5 Mya)] and the clade containing *R. everetti*, *Tarsomys*, and *Limnomys* [MRCA, 2.7 Mya (2.5–3.1 Mya); Philippine diversification, 2.0 Mya (1.5–2.5 Mya)]. The single colonization of the Sahul region comprises a clade of species of *Rattus* [MRCA, 2.4 Mya (2.0–2.9 Mya); Sahul diversification, 1.4 Mya (1.1–1.7 Mya)]. There was also one major range expansion and diversification in Wallacea of the clade containing *Paruromys*, *Taeromys*, and the Moluccan *Halmaheramys* [MRCA, 3.1 Mya (2.5–3.6 Mya); Wallacea diversification, 2.76 Mya (2.30–3.16 Mya)]. We inferred two recent colonizations of Wallacea from both Sahulian and Southeast Asian ancestors that led to the speciation of *R. morotaiensis* in the North Moluccas [MRCA, 1.4 Mya (1.1–1.7 Mya); Wallacea diversification, 1.1 Mya (0.8.1–1.4 Mya)] and *Rattus hoffmanni* (Matschie, 1901) in Sulawesi [MRCA, 1.4 Mya (1.1–1.8 Mya); Wallacea diversification, 1.0 Mya (0.7–1.4 Mya)], respectively.

MORPHOLOGICAL ANALYSIS

A clade containing the Sundaic *Sundamys*, Philippine *Bullimus*, Sulawesian *Bunomys*, *Taeromys*, and *Paruromys*, and Moluccan *Halmaheramys* was recovered in our analyses of DNA sequences (clade G in Fig. 2). Within this cluster, *H. bokimekot* gen. et sp. nov. was sister to the Sulawesian taxa *Bunomys*, *Taeromys*, and *Paruromys* (clade H in Fig. 2). In our morphological comparisons, we compare *Halmaheramys* in greatest detail with these three closely related genera. Descriptive statistics for external measurements are presented in Table 1. Comparisons of craniodental measurements for *H. bokimekot* gen. et sp. nov. and

Figure 2. A, maximum-likelihood topology for the Rattini division produced from the combined analysis. Labelled clades are discussed in the text. Numbers at nodes represent maximum-likelihood (ML) bootstrap support values > 70%, Bayesian posterior probabilities from MrBayes (PP1) and posterior probabilities computed by Phylobayes (PP2). Where possible, voucher numbers are indicated for each specimen used in this study. Murinae clades are highlighted using the full ML topology on the left of the figure. Colours on the tree indicate geographical occurences (see legends). The Halmahera map and direction of colonization are indicated on the right side of the topology (blue and green represent colonization from Southeast Asia and Sahul, respectively). B, distribution of biodiversity in the Rattini. The colour gradient represents species richness: a warmer colour indicates a higher richness. Black corresponds to areas where the group is not present.

Table 2. Cross-validation of the fossil constraints through molecular dating generated from the concatenated mitochondrial + nuclear data set

MRCA (median fossil age)	ALLCal PHL 10.0–22.9 Mean (Min–Max)	ALLCal cMUR 10.0–22.9 Mean (Min–Max)	WithoutCal1 Mean (Min–Max)
Core Murinae	11.6 (10.2–13.0)	12.1 (10.9–13.6)	11.8 (10.4–13.7)
Antemus/Progonomys (12.1 Mya)	10.1 (9.2–11.3)	10.5 (9.7–11.6)	10.3 (9.2–11.6)
Apodemurini (11 Mya)	9.3 (8.5–10.2)	9.5 (8.7–10.5)	9.4 (8.5–10.5)
Apodemus/Sylvaemus (7 Mya)	6.3 (5.8–7.0)	6.4 (5.8–7.2)	6.4 (5.8–7.2)
Mus (5.7 Mya)	5.5 (4.6–9.6)	5.6 (4.7–6.6)	5.6 (4.7–6.6)
Arvicanthini (6 Mya)	7.2 (6.2–8.1)	7.4 (4.4–8.3)	7.2 (6.3–8.3)
Sahul Hydromyini (3.4 Mya)	6.8 (5.9–7.7)	7.0 (6.0–7.9)	6.9 (5.9–7.9)
A Rattini clade	8.7 (7.5–9.9)	8.9 (7.7–10.2)	8.8 (7.5–10.2)
B	7.0 (6.0–8.0)	7.2 (6.2–8.2)	7.0 (6.0–8.2)
C *Maxomys + Crunomys* division	4.8 (3.8–5.9)	4.9 (3.9–6.0)	4.8 (3.8–6.0)
D	5.9 (5.0–6.8)	6.1 (5.2–7.0)	6.0 (5.1–7.0)
E *Dacnomys* division	5.1 (4.2–6.0)	5.3 (4.4–6.2)	5.1 (4.2–6.0)
F *Rattus* division	4.5 (3.8–5.4)	4.6 (3.9–5.4)	4.6 (3.8–5.4)
G	3.5 (3.0–4.1)	3.6 (3.1–4.2)	3.6 (3.0–4.2)
H	3.1 (2.5–3.6)	3.1 (2.6–3.7)	3.1 (2.5–3.6)
I	2.4 (1.9–2.8)	2.4 (1.9–2.9)	2.4 (1.9–2.9)
J	2.9 (2.5–3.3)	3.0 (2.5–3.4)	3.0 (2.5–3.4)
K	1.4 (1.1–1.7)	1.5 (1.1–1.8)	1.5 (1.1–1.9)
L	1.2 (0.8–1.6)	1.2 (0.8–1.6)	2.1 (1.6–2.6)
M	2.5 (2.0–2.9)	2.5 (2.1–3.0)	2.5 (2.0–3.0)
N	2.0 (1.5–2.5)	2.1 (1.6–2.6)	2.1 (1.6–2.6)

Letters referred to the nodes in Figure 2. The mean age of each node is given in million years ago (Mya), together with the lower and upper bounds of the 95% confidence intervals issued from the Bayesian relaxed molecular clock analysis. The fossil constraints are described in the Material and methods and Figure 3. Values pertaining to the cross-validation are set in bold. MRCA, most recent common ancestor. The fossil constraints are as follows: ALLCalMur, all six calibrations, with calibration 1 on the Murinae divergence; ALLCalcMur, all six calibrations, with calibration 1 on the core Murinae divergence; WithoutCal1, calibrations 2–5, without calibration 1.

species of *Bunomys*, *Paruromys*, and *Taeromys* are presented in Tables 3–5. The results of the principal components analyses are shown in Figures 5 and 6 (PCA). Between 351 and 641 specimens of genera belonging to clade I in our tree (Fig. 2) were analysed together with *Halmaheramys*. Loading valuess for the first two components of each PCA are presented in Tables 6 and 7. Based on our phylogenetic results, morphometric comparisons, biogeographical considerations, and examinations of qualitative morphology, we recognize *Halmaheramys* as a new genus, as described and discussed here.

DISCUSSION

TAXONOMY

Family muridae
*Halmaheramys* Fabre, Pagès, Musser, Fitriana, Semiadi & Helgen gen. nov.

Type species: Halmaheramys bokimekot Fabre, Pagès, Musser, Fitriana, Semiadi & Helgen sp. nov.

Etymology: Halmaheramys is named after its geographical provenance in the North Moluccas, as so far it is the only known murine genus that is endemic to the island of Halmahera.

Diagnosis: Based upon analyses of DNA sequences, *Halmaheramys* is a member of the *Rattus* division within the tribe Rattini (*sensu* Lecompte *et al.*, 2008; Aplin & Helgen, 2010), subfamily Murinae, family Muridae (as delimited by Carleton & Musser, 1984; Musser & Carleton, 2005), and a Moluccan representative of a monophyletic Indo-Pacific clade that also contains the Sundaic *Sundamys*, Philippine *Bullimus*, and Sulawesian *Bunomys*, *Paruromys*, and *Taeromys* (Fig. 2). *Halmaheramys* is distinguished from these genera, as well as all other murine genera
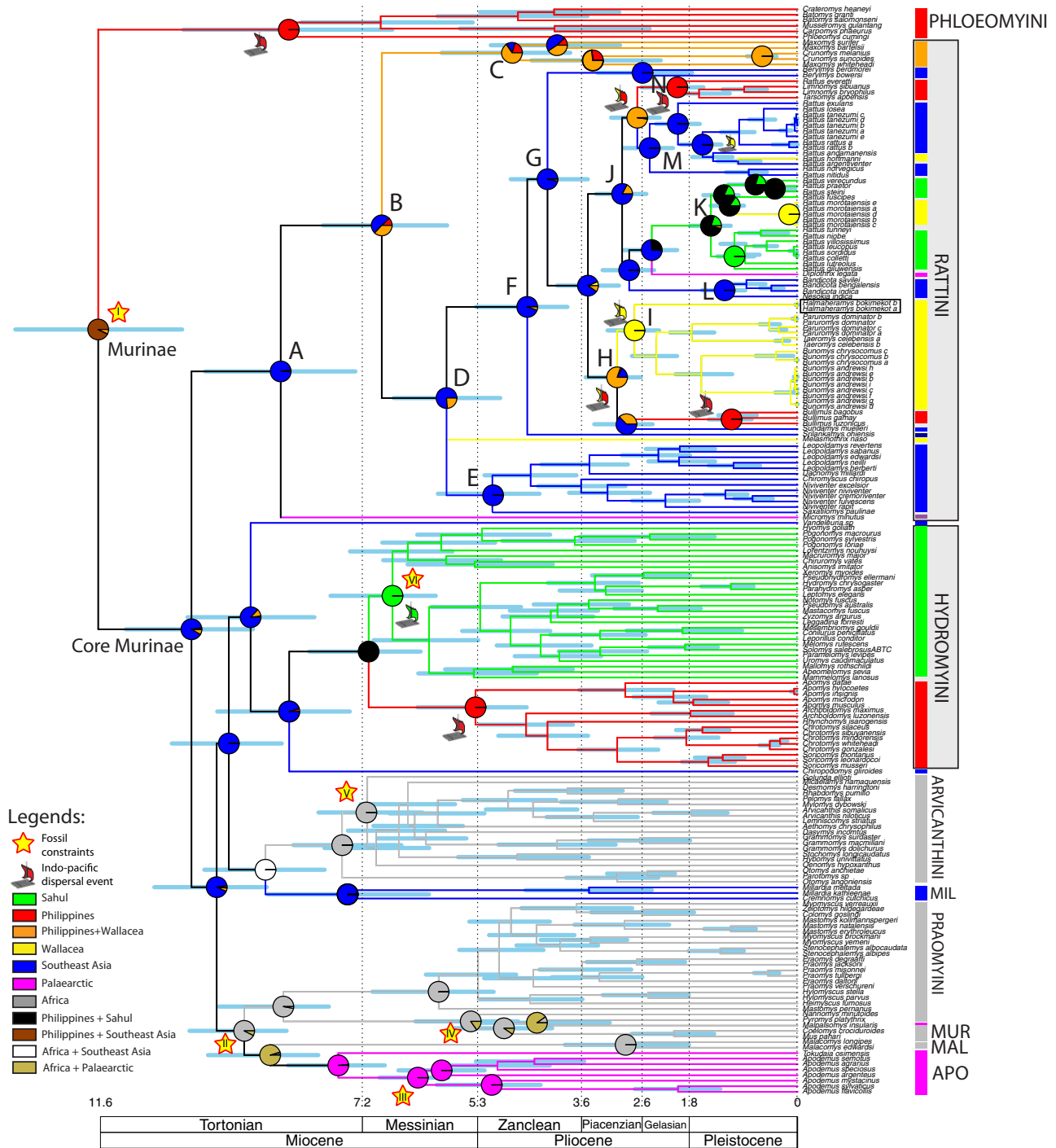
Figure 3. Ancestral area reconstructions for the subfamily Murinae. The tree is a chronogram (uncorrelated log-normal molecular clock) based on a BEAST Markov chain Monte Carlo (MCMC) analysis of the combined data set. Maximum-likelihood ancestral area reconstructions were conducted on 1000 randomly sampled trees (allowing for alternative topologies to be included) from the posterior distribution of the BEAST analysis. The distribution for each taxon is indicated to the right of the taxon names. Coloured pies indicate the origin of a given node. The raft symbol indicates inferred dispersal and colonization routes used by the members of the Indo-Pacific Murinae. The stars indicate the fossil calibration points used for absolute dating (see Material and methods).
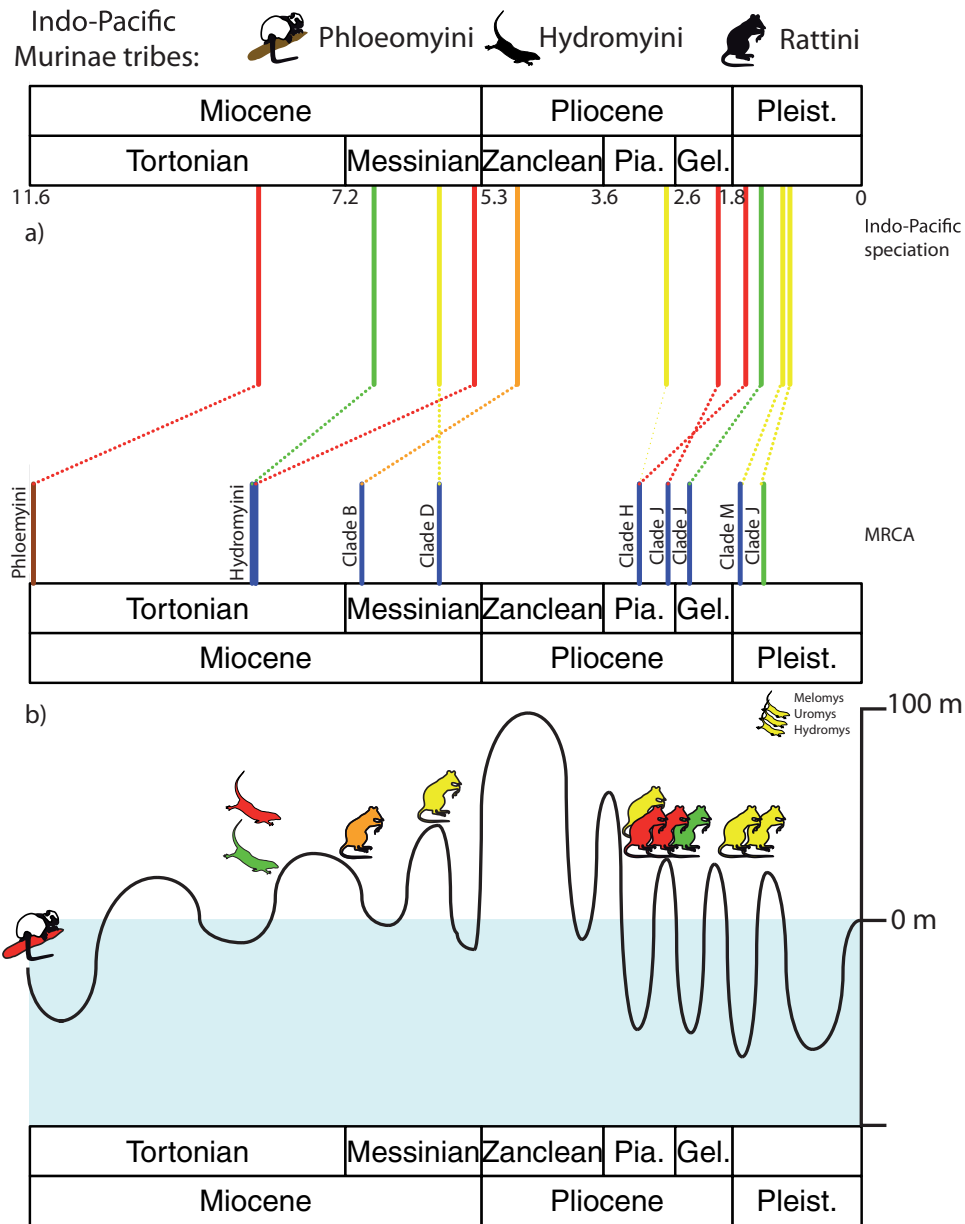
Figure 4. A, summary of the geographic and temporal origins of Indo-Pacific Murinae lineages. The bars on the geological time scale represent the dates of divergence of Indo-Pacific lineages from the most recent common ancestor of sister lineages (MRCA; bottom), and of the first diversification event on each Indo-Pacific archipelago (top). Each colour represents the most likely biogeographical origin (see Lagrange results in Fig. 3). B, diagram of eustatic sea level fluctuations in Southeast Asia, redrawn from Haq *et al*. (1987). The rodent icons represent the main lineages of Indo-Pacific Murinae. The coloirs refer to biogeographic areas.

described, by the following combination of morphological traits: (1) medium body size and terrestrial habitus; (2) dorsal pelage covering the head and body, harsh, thick, and dark-brownish grey, with scattered bristly and spiny hairs; (3) ventral coat coarse and whitish grey, demarcation between upper parts and under parts conspicuous; (4) moderately long muzzle, with ears that are dark-brownish grey; (5) a tail that is appreciably shorter than the head–body length (mean value of TL/HB = 81%), with epidermal scales square and large (with 9–11 scale rings per cm near base of tail); annuli overlapping; three short harsh/spiny hairs associated with each scale; and all surfaces of the tail brown, with a short white tip; (6) digits and dorsal surfaces of carpal and metacarpal regions white; palmar surface adorned with usual

Table 3. Descriptive statistics for cranial and dental measurements (mm) for six species of *Bunomys* and ***Halmaheramys bokimekot*** gen. et sp. nov.

Variable	*Bunomys*						*Halmaheramys* gen. nov.
	B. fratrorum	*B. andrewsi*	*B. penitus*	*B. prolatus*	*B. coelestis*	*B. chrysocomus*	*H. bokimekot* gen. et sp. nov.
N	100	98	185	8	18	232	6
ONL	44.0 ± 1.14 (41.5–46.5)	41.0 ± 2.04 (37.1–45.5)	43.0 ± 1.24 (39.3–46.1)	41.8 ± 1.03 (40.4–43.2)	40.2 ± 0.92 (37.6–41.8)	38.3 ± 1.12 (35.8–41.1)	38.3 ± 0.92 (36.9–39.2)
ZB	20.9 ± 0.90 (18.2–22.9)	20.0 ± 1.04 (17.9–22.2)	19.6 ± 0.70 (17.0–21.4)	17.8 ± 0.38 (17.2–18.3)	18.7 ± 0.64 (17.2–20.4)	18.1 ± 0.64 (16.3–19.8)	16.9 ± 0.64 (16.1–17.9)
IB	6.2 ± 0.31 (5.5–7.0)	6.6 ± 0.24 (6.1–7.3)	6.8 ± 0.25 (6.1–8.3)	7.1 ± 0.23 (6.9–7.4)	6.6 ± 0.24 (6.2–7.2)	6.4 ± 0.23 (5.8–7.2)	6.3 ± 0.28 (5.9–6.7)
LR	15.2 ± 0.56 (13.9–16.6)	14.6 ± 1.02 (12.2–17.2)	16.1 ± 0.66 (14.6–18.1)	15.7 ± 0.61 (14.7–16.4)	14.7 ± 0.56 (13.6–15.7)	13.5 ± 0.59 (12.0–15.1)	13.5 ± 0.56 (12.7–14.2)
BR	8.0 ± 0.38 (7.2–9.0)	7.4 ± 0.50 (6.5–8.9)	8.0 ± 0.37 (7.0–9.0)	6.7 ± 0.36 (6.1–7.1)	6.8 ± 0.47 (5.7–7.6)	6.8 ± 0.36 (5.6–7.7)	6.4 ± 0.31 (6.1–6.8)
BBC	16.3 ± 0.41 (15.3–16.3)	16.2 ± 0.48 (15.0–17.9)	16.5 ± 0.45 (15.1–17.7)	16.3 ± 0.37 (15.7–16.9)	15.7 ± 0.41 (14.9–16.3)	15.5 ± 0.41 (14.2–16.8)	15.2 ± 0.36 (14.8–15.7)
HBC	12.2 ± 0.43 (11.3–13.1)	11.6 ± 0.46 (10.6–13.0)	11.8 ± 0.36 (10.9–12.7)	11.4 ± 0.19 (11.0–11.6)	11.6 ± 0.24 (11.1–12.1)	10.8 ± 0.38 (10.0–12.1)	11.7 ± 0.36 (11.3–12.3)
BZP	3.9 ± 0.32 (3.1–4.6)	3.7 ± 0.42 (2.9–4.6)	3.0 ± 0.22 (2.4–3.6)	2.8 ± 0.10 (2.6–2.9)	3.6 ± 0.19 (3.3–4.0)	3.2 ± 0.26 (2.6–3.9)	3.2 ± 0.22 (2.9–3.5)
LD	11.4 ± 0.51 (10.2–13.1)	10.9 ± 0.76 (9.5–12.6)	11.3 ± 0.53 (10.0–12.8)	11.5 ± 0.56 (10.7–12.3)	12.1 ± 0.54 (11.0–13.1)	10.2 ± 0.54 (8.8–12.0)	9.9 ± 0.42 (9.4–10.6)
PPL	15.4 ± 0.60 (13.9–16.8)	14.5 ± 0.87 (12.5–16.2)	14.6 ± 0.54 (12.9–16.1)	14.6 ± 0.51 (13.8–15.2)	14.3 ± 0.53 (13.1–15.2)	13.5 ± 0.58 (12.2–15.0)	13.3 ± 0.45 (12.8–13.9)
LBP	8.0 ± 0.46 (6.9–9.8)	7.8 ± 0.51 (6.8–9.9)	8.8 ± 0.43 (7.4–9.8)	8.7 ± 0.35 (8.3–9.20)	8.1 ± 0.39 (7.5–8.8)	7.5 ± 0.40 (6.2–8.4)	7.1 ± 0.30 (6.6–7.4)
BBPM1	3.8 ± 0.27 (3.3–4.5)	3.8 ± 0.33 (2.9–4.6)	3.6 ± 0.28 (2.9–4.3)	3.7 ± 0.15 (3.4–3.9)	3.7 ± 0.20 (3.3–4.0)	3.8 ± 0.26 (3.1–4.5)	3.2 ± 0.21 (3.0–3.5)
BMF	3.5 ± 0.26 (3.0–4.3	3.2 ± 0.27 (2.6–4.0)	3.6 ± 0.28 (2.8–4.4)	2.8 ± 0.14 (2.6–3.0)	2.8 ± 0.18 (2.5–3.2)	2.9 ± 0.24 (2.4–3.7)	3.6 ± 0.18 (3.3–3.8)
LIF	7.3 ± 0.42 (6.2–8.3)	8.0 ± 0.57 (6.8–9.5)	8.1 ± 0.47 (7.0–9.2)	6.7 ± 0.29 (6.3–7.1)	6.9 ± 0.36 (6.5–7.7)	6.3 ± 0.37 (5.2–7.2)	6.0 ± 0.15 (5.8–6.1)
BIF	2.9 ± 0.16 (2.5–3.3)	3.0 ± 0.23 (2.5–3.6)	3.0 ± 0.20 (2.5–3.4)	2.3 ± 0.13 (2.1–2.5)	2.2 ± 0.15 (1.9–2.5)	2.5 ± 0.17 (2.0–3.1)	2.3 ± 0.08 (2.2–2.4)
LB	6.5 ± 0.20 (6.1–7.0)	6.5 ± 0.34 (5.7–7.4)	6.8 ± 0.30 (6.0–8.0)	6.9 ± 0.30 (6.5–7.3)	6.3 ± 0.22 (58–6.8)	6.4 ± 0.24 (5.7–7.0)	5.3 ± 0.16 (5.2–5.6)
CLM1–3	7.6 ± 0.26 (6.8–8.1)	7.2 ± 0.31 (6.5–8.0)	7.8 ± 0.26 (7.0–8.4)	6.5 ± 0.17 (6.3–6.8)	6.1 ± 0.23 (5.7–6.6)	6.2 ± 0.23 (5.7–6.8)	6.6 ± 0.16 (6.4–6.8)
BM1	2.4 ± 0.10 (2.2–2.7)	2.3 ± 0.10 (2.0–2.5)	2.5 ± 0.11 (2.2–2.8)	2.2 ± 0.09 (2.0–2.3)	2.0 ± 0.10 (1.8–2.1)	2.0 ± 0.09 (1.8–2.3)	2.0 ± 0.08 (1.9–2.1)

Mean ± 1 SD and observed range (in parentheses) are listed. Sexes are combined in the samples. Abbreviations: BBC, breadth of the braincase; BBPM1, breadth of the bony plate at first molar; BIF, breadth of the incisive foramen; BM1, breadth of first upper molar; BMF, breadth of the mesopterygoid fossa; BR, breadth of the rostrum; BZP, breadth of the zygomatic plate; CLM1–3, crown length of the maxillary molar row; HBC, height of the braincase; IB, least interorbital breadth; LB, length of auditory bulla; LBP, length of bony palate; LD, length of the diastema; LIF, length of the incisive foramen; LR, length of the rostrum; ONL, occipitonasal length; PPL, postpalatal length; ZB, greatest zygomatic breadth.

Table 4. Descriptive measurements for cranial and dental measurements (mm) for ***Halmaheramys bokimekot* gen. et sp. nov.** and seven species of *Taeromys*
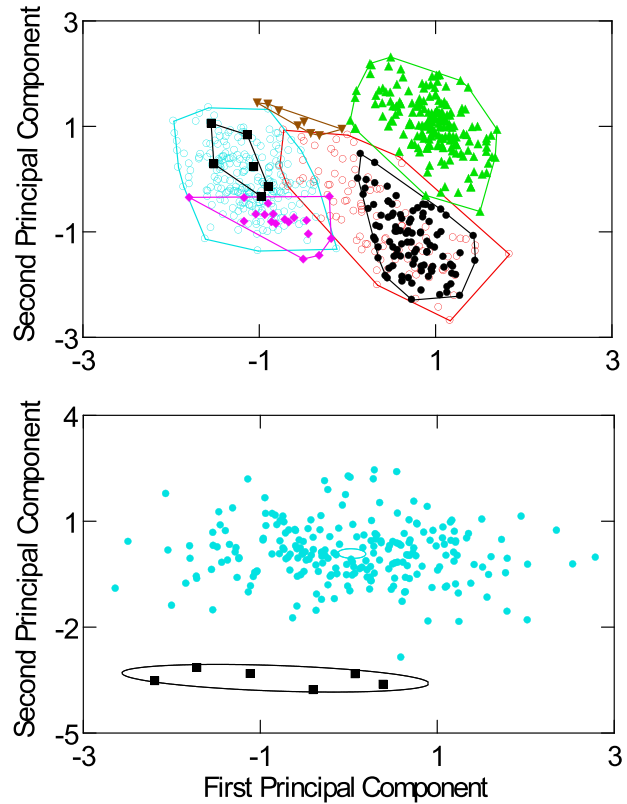
	Halmaheramys gen. nov.	*Taeromys*						
Variable	**H. bokimekot gen. et sp. nov.**	*T. arcuatus*	*T. taerae*	*T. hamatus*	*T. celebensis*	*T. callitrichus*	*T. microbullatus*	*T. punicans*
N	6	7	5	12	53	11	2	1
ONL	38.3 ± 0.92 (36.9–39.2)	50.5 ± 0.67 (49.8–51.8)	50.8 ± 0.70 (50.3–52.0)	46.0 ± 1.59 (43.4–48.4)	50.0 ± 1.95 (44.6–53.3)	50.1 ± 1.70 (46.6–52.3)	50.1 ± 0.14 (50.0–50.2)	45.9
ZB	16.9 ± 0.64 (16.1–17.9)	22.0 ± 0.33 (21.6–22.7)	23.7 ± 0.76 (22.6–24.5)	22.7 ± 0.68 (21.8–24.3)	24.2 ± 1.06 (21.7–26.4)	24.6 ± 0.87 (22.6–25.8)	24.7 ± 0.42 (24.4–25.0)	22.0
IB	6.3 ± 0.28 (5.9–6.7)	6.9 ± 0.18 (6.6–7.1)	6.8 ± 0.21 (6.5–7.0)	6.8 ± 0.26 (6.4–7.4)	6.9 ± 0.33 (6.3–7.8)	6.9 ± 0.21 (6.7–7.3)	6.8 ± 0.07 (6.7–6.8)	6.3
LR	13.5 ± 0.56 (12.7–14.2)	19.1 ± 0.24 (18.8–19.5)	17.9 ± 0.49 (17.2–18.4)	15.9 ± 0.68 (14.9–16.9)	15.8 ± 0.90 (13.7–18.6)	16.3 ± 1.09 (14.8–18.2)	16.9 ± 0.42 (16.6–17.2)	15.0
BR	6.4 ± 0.31 (6.1–6.8)	8.0 ± 0.34 (7.6–8.4)	8.4 ± 0.30 (8.0–8.8)	8.2 ± 0.48 (7.8–9.3)	9.2 ± 0.49 (8.0–10.3)	8.6 ± 0.37 (8.2–9.2)	9.1 ± 0.14 (9.0–9.2)	7.4
BBC	15.2 ± 0.36 (14.8–15.7)	18.0 ± 0.35 (17.6–18.5)	18.6 ± 0.35 (18.2–19.1)	17.4 ± 0.52 (16.5–18.3)	19. ± 0.62 (18.1–20.5)	19.4 ± 0.55 (18.4–20.3)	18.7 ± 0.42 (18.4–19.0)	17.8
HBC	11.7 ± 0.36 (11.3–12.3)	13.1 ± 0.45 (12.4–13.5)	12.4 ± 0.22 (12.2–12.7)	12.2 ± 0.38 (11.4–12.8)	13.6 ± 0.49 (12.6–14.5)	13.9 ± 0.40 (13.3–14.6)	14.2 ± 0.57 (13.8–14.6)	13.4
BZP	3.2 ± 0.22 (2.9–3.5)	5.8 ± 0.48 (5.2–6.7)	5.7 ± 0.19 (5.4–5.9)	5.3 ± 0.37 (4.9–6.2)	5.1 ± 0.41 (4.2–6.0)	5.5 ± 0.35 (4.9–6.2)	5.5 ± 0.35 (4.9–6.2)	5.0
LD	9.9 ± 0.42 9.4–10.6)	13.4 ± 0.29 (13.0–13.9)	13.5 ± 0.23 (13.1–13.7	12.2 ± 0.70 (11.2–13.5)	13.6 ± 0.72 (11.9–15.0)	13.2 ± 0.99 (11.7–14.7)	14.5 ± 0.35 (14.2–14.7)	11.1
PPL	13.3 ± 0.45 (12.8–13.9)	17.9 ± 0.52 (17.2–18.6)	17.1 ± 0.22 (16.9–17.4)	15.1 ± 0.85 (14.0–16.5)	18.1 ± 0.97 (15.7–20.1)	17.7 ± 0.51 (17.0–18.8)	17.9 ± 0.21 (17.7–18.0)	14.8
LBP	7.1 ± 0.30 (6.6–7.4)	10.3 ± 0.39 (9.9–10.8)	9.7 ± 0.39 (9.1–10.1)	8.9 ± 0.34 (8.3–9.4)	10.3 ± 0.54 (8.9–11.6)	10.9 ± 0.65 (10.1–12.1)	11.0 ± 0.42 (10.7–11.3)	9.7
BBPM1	3.2 ± 0.21 (3.0–3.5)	3.4 ± 0.34 (2.8–4.0)	3.9 ± 0.14 (3.7–4.1)	3.6 ± 0.23 (3.1–3.9)	4.1 ± 0.35 (3.4–4.8)	3.4 ± 0.38 (2.8–4.0)	4.0 ± 0.07 (3.9–4.0)	3.5
BMF	3.6 ± 0.18 (3.3–3.8)	3.4 ± 0.20 (3.2–3.8)	3.7 ± 0.30 (3.3–4.1)	2.9 ± 0.16 (2.6–3.2)	3.9 ± 0.30 (3.2–4.7)	3.3 ± 0.13 (3.1–3.5)	3.3 ± 0.14 (3.2–3.4)	3.1
LIF	6.0 ± 0.15 (5.8–6.1)	8.1 ± 0.36 (7.2–8.6)	9.1 ± 0.10 (9.0–9.2)	8.5 ± 0.53 (7.7–9.2)	8.2 ± 0.65 (6.0–9.5)	7.8 ± 0.54 (6.8–8.5)	7.5 ± 0.28 (7.3–7.7)	6.6
BIF	2.3 ± 0.08 (2.2–2.4)	2.8 ± 0.17 (2.6–3.0)	3.0 ± 0.11 (2.9–3.2)	3.1 ± 0.15 (2.8–3.3)	3.1 ± 0.26 (2.6–3.7)	2.8 ± 0.20 (2.5–3.1)	2.7 ± 0.00	2.6
LB	5.3 ± 0.16 (5.2–5.6)	7.3 ± 0.13 (7.1–7.4)	6.8 ± 0.13 (6.6–6.9)	6.2 ± 0.28 (5.5–6.6)	7.6 ± 0.34 (7.1–8.8)	6.7 ± 0.52 (5.5–7.4)	6.7 ± 0.21 (6.5–6.8)	7.0
CLM1–3	6.6 ± 0.16 (6.4–6.8)	9.0 ± 0.33 (8.5–9.4)	8.7 ± 0.08 (8.6–8.8)	8.4 ± 0.20 (7.9–8.6)	8.5 ± 0.28 (8.0–9.1)	9.6 ± 0.41 (8.7–10.0)	8.9 ± 0.21 (8.7–9.0)	8.6
BM1	2.0 ± 0.08 (1.9–2.1)	2.5 ± 0.10 (2.4–2.7)	2.5 ± 0.05 (2.4–2.5)	2.4 ± 0.11 (2.2–2.6)	2.7 ± 0.10 (2.5–2.8)	3.0 ± 0.16 (2.7–3.2)	2.8 ± 0.07 (2.7–2.8)	2.6

Mean ± SD and observed range (in parentheses) are listed. Sexes are combined in the samples greater than N = 1. Abbreviations: BBC, breadth of the braincase; BBPM1, breadth of the bony plate at first molar; BIF, breadth of the incisive foramen; BM1, breadth of first upper molar; BMF, breadth of the mesopterygoid fossa; BR, breadth of the rostrum; BZP, breadth of the zygomatic plate; CLM1–3, crown length of the maxillary molar row; HBC, height of the braincase; IB, least interorbital breadth; LB, length of auditory bulla; LBP, length of bony palate; LD, length of the diastema; LIF, length of the incisive foramen; LR, length of the rostrum; ONL, occipitonasal length; PPL, postpalatal length; ZB, greatest zygomatic breadth.

Table 5. Descriptive statistics for cranial and dental measurements (mm) for ***Halmaheramys bokimekot* gen. et sp. nov.** and *Paruromys dominator*

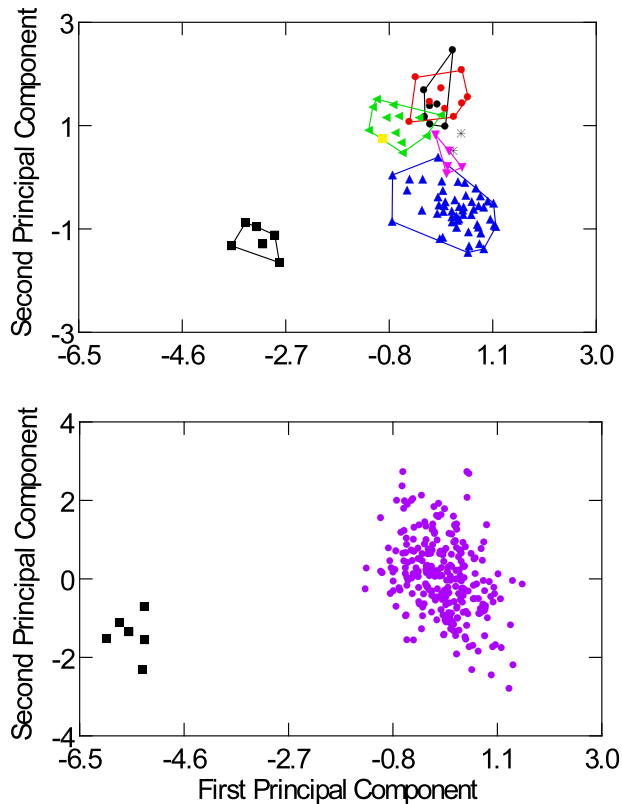| Variable	*Halmaheramys bokimekot* gen. et sp. nov.	*Paruromys dominator*
N	6	260
ONL	38.3 ± 0.92	58.1 ± 1.93
	(36.9–39.2)	(52.9–63.2)
ZB	16.9 ± 0.64	26.9 ± 0.95
	(16.1–17.9)	(24.2–29.5)
IB	6.3 ± 0.28	7.8 ± 0.39
	(5.9–6.7)	(6.8–8.9)
LR	13.5 ± 0.56	19.5 ± 0.93
	(12.7–14.2)	(15.5–22.2)
BR	6.4 ± 0.31	9.5 ± 0.47
	(6.1–6.8)	(8.3–11.3)
BBC	15.2 ± 0.36	20.6 ± 0.54
	(14.8–15.7)	(19.1–22.0)
HBC	11.7 ± 0.36	14.5 ± 0.52
	(11.3–12.3)	(13.2–16.3)
BZP	3.2 ± 0.22	7.5 ± 0.69
	(2.9–3.5)	(5.8–10.0)
LD	9.9 ± 0.42	15.1 ± 0.72
	9.4–10.6)	(13.2–17.3)
PPL	13.3 ± 0.45	19.2 ± 0.91
	(12.8–13.9)	(17.4–21.3)
LBP	7.1 ± 0.30	13.6 ± 0.75
	(6.6–7.4)	(12.0–15.9)
BBPM1	3.2 ± 0.21	4.5 ± 0.36
	(3.0–3.5)	(2.9–5.4)
BMF	3.6 ± 0.18	3.5 ± 0.27
	(3.3–3.8)	(2.8–4.7)
LIF	6.0 ± 0.15	7.6 ± 0.53
	(5.8–6.1)	(6.1–9.8)
BIF	2.3 ± 0.08	2.9 ± 0.24
	(2.2–2.4)	(2.1–3.6)
LB	5.3 ± 0.16	7.3 ± 0.31
	(5.2–5.6)	(6.5–8.7)
CLM1-3	6.6 ± 0.16	9.2 ± 0.30
	(6.4–6.8)	(8.4–10.2)
BM1	2.0 ± 0.08	2.8 ± 0.12
	(1.9–2.1)	(2.5–3.1)

Mean ± SD and observed range (in parentheses) are listed. Sexes are combined in the samples. Abbreviations: BBC, breadth of the braincase; BBPM1, breadth of the bony plate at first molar; BIF, breadth of the incisive foramen; BM1, breadth of first upper molar; BMF, breadth of the mesopterygoid fossa; BR, breadth of the rostrum; BZP, breadth of the zygomatic plate; CLM1–3, crown length of the maxillary molar row; HBC, height of the braincase; IB, least interorbital breadth; LB, length of auditory bulla; LBP, length of bony palate; LD, length of the diastema; LIF, length of the incisive foramen; LR, length of the rostrum; ONL, occipitonasal length; PPL, postpalatal length; ZB, greatest zygomatic breadth.

Figure 5. Specimen scores projected on first and second principal components extracted from principal component analysis. Upper panel: the sample of ***Halmaheramys bokimekot* gen. et sp. nov.** (filled black square; *N* = 6) is compared with samples of six species of *Bunomys*: *B. andrewsi* (empty red circle; *N* = 98); *B. chrysocomus* (empty cyan circle; *N* = 232); *B. coelestis* (filled magenta diamond; *N* = 18); *B. fratrorum* (filled black circle; *N* = 100); *B. penitus* (filled green upright triangle; *N* = 185); and *B. prolatus* (filled brown inverted triangle; *N* = 8). Lower panel: samples of ***Halmaheramys bokimekot* gen. et sp. nov.** (filled black square; *N* = 6) and *Bunomys chrysocomus* (filled cyan circle; *N* = 232) are contrasted. Ellipses outline 95% confidence limits for cluster centroids. See Table 6 for correlations of variables and percent variance for both graphs.

number of tubercles found in murines (three interdigitals, a thenar, and a hypothenar); hindfoot elongate with full complement of plantar tubercles (four interdigitals, a thenar, and a hypothenar); front claws moderately long; (7) three pairs of teats, one postaxillary and two inguinal $(0 + 1 + 2 = 6)$; (8) rostrum moderately long and narrow; interorbital and postorbital margins bounded by low and inconspicuous ridges; zygomatic arches arc slightly from sides of braincase; posterior zygomatic root situated low on braincase; braincase moderately wide and deep; occiput deep, no cranial flexion; (9) zygomatic plate

Figure 6. Specimen scores projected on first and second principal components extracted from principal component analysis. Upper panel: the sample of ***Halmaheramys bokimekot* gen. et sp. nov.** (solid black square; $N = 6$) is compared with samples of seven species of *Taeromys*: *T. arcuatus* (black circle; $N = 7$); *T. callitrichus* (red circle; $N = 11$); *T. microbullatus* (asterisk; $N = 2$); *T. punicans* (yellow square; $N = 1$); *T. celebensis* (upright blue triangle; $N = 53$); *T. hamatus* (left-pointing green triangle; $N = 12$); and *T. taerae* (inverted magenta triangle; $N = 5$). Lower panel: samples of ***Halmaheramys bokimekot* gen. et sp. nov.** (black square; $N = 6$) and *Paruromys dominator* (violet circle; $N = 260$) are compared and contrasted. See Table 7 for correlations of variables and percent variance for both graphs.

narrow, its anterior margin barely projecting beyond dorsal maxillary root of zygomatic arch, and its posterior edge even with the anterior third of the first molar; (10) squamosal intact, not perforated by a subsquamosal foramen; (11) alisphenoid struts absent; (12) incisive foramina moderately long and wide, their posterior borders even with anterior alveolar margins of first molars; (13) molar rows diverge posteriorly; bony palate short, with its posterior margin even with back faces of third molars; palatal surface with moderately deep palatine grooves; posterior palatine foramina at level where second and third molar touch; (14) sphenopalatine vacuities mod-

erately long and narrow; (15) pterygoid plates wide, with moderately deep pterygoid fossa, small sphenopterygoid openings; (16) ectotympanic (auditory) bulla small relative to skull size; capsule incompletely covering periotic; posterodorsal wall of carotid canal formed by periotic and not bullar capsule; (17) large stapedial foramen, no sphenofrontal foramen or squamosal–alisphenoid groove, indicating a carotid arterial pattern widespread within Murinae (character state 2 of Carleton, 1980; pattern 2 described by Voss, 1988); (18) dentary stocky, short and thick ramus between incisor and molar row, high ascending ramus, large coronoid and condyloid processes, end of alveolar capsule forming modest labial bulge level with base of coronoid process; (19) upper and lower incisors with orange enamel and ungrooved anterior faces, uppers emerge from the rostrum at a right angle (orthodont configuration), each lower incisor is stocky, with short wear facets; (20) each first upper molar (maxillary) with five roots, the second with four, and the third with three, each first lower (mandibular) molar with four, the second and third molars each with three; (21) molars brachydont and narrow; cusp rows forming simple cuspidate occlusal patterns; third molar small relative to others in toothrow; (22) first and second rows of cusps on first upper molars arcuate; cusps broadly coalesced within each row; anterior row of second molar shaped like second row of first molar; (23) no cusp t7 or posterior cingulum on upper molars, and no other occlusal embellishments (such as an enamel ridge projecting from anterolingual surface of cusp t8 anteriorly to posterior margin of lingual cusp t4, a labial enamel ridge connecting anterolabial margin of cusp t9, with posterolabial margin of cusp t6, or a comparable but shorter ridge projecting from the anterior surface of cusp t5 to meet the posterior margin of cusp t3 near the cingulum, all typical of some other murines with more complicated enamel occlusal patterns (the New Guinea *Coccymys* is an example; Musser & Lunde, 2009), cusp t3 missing from second and third molars; (24) anteroconid formed of large anterolingual and anterolabial cusps broadly fused into single lamina, elliptical or oblong in cross section; anterocentral cusp absent, anterolabial cusp missing from second and third lower molars, anterior labial cusplets not present on first and second lower molars, but posterior labial cusplet present on some specimens, posterior cingulum elliptical in cross section; (25) at least three young per litter.

Description: The genus is currently monotypic; see description for the species, below. *Composition:* The type species and only known member of *Halmaheramys* is *H. bokimekot* sp. nov. Additional species of *Halmaheramys* are represented in the subfossil

Table 6. Results of principal component analyses comparing ***Halmaheramys bokimekot* gen. et sp. nov.** with: (1) six species of *Bunomys* and (2) *Bunomys chrysocomus*

| | Correlations (loadings) | | | |
| | *Halmaheramys* and species of *Bunomys* | | *Halmaheramys* and *Bunomys chrysocomus* | |
Variable	PC1	PC2	PC1	PC2
ONL	0.93***	−0.12**	0.79***	0.16*
ZB	0.83***	−0.40***	0.73***	0.26***
IB	0.34***	0.31***	0.44***	0.04
LR	0.89***	0.13***	0.74***	0.05
BR	0.89***	−0.12**	0.73***	0.09
BBC	0.77***	0.09*	0.34***	0.18**
HBC	0.78***	−0.14***	0.21***	−0.08
BZP	0.18***	−0.95***	0.50***	−0.21***
LD	0.75***	−0.18***	0.73***	0.32***
PPL	0.77***	−0.36***	0.72***	−0.01
LBP	0.70***	0.29***	0.48***	0.22***
BBPM1	0.09*	−0.51***	0.71***	0.30***
BMF	0.81***	0.13***	0.48***	−0.82***
LIF	0.87***	0.07	0.29***	0.37***
BIF	0.86***	−0.06	0.47***	0.01
LB	0.50***	0.21***	0.31***	0.55***
CLM1–3	0.92***	0.14***	0.14*	−0.18**
BM1	0.86***	0.24***	0.15*	−0.05
Eigenvalue	0.083	0.021	0.015	0.007
% Variance	58.3	14.8	29.4	14.4

Correlations (loadings) of 16 cranial and two dental log-transformed variables are based on 641 specimens representing seven species; see Figure 5. ***$P \leq 0.001$; **$P \leq 0.01$; *$P \leq 0.05$. Abbreviations: BBC, breadth of the braincase; BBPM1, breadth of the bony plate at first molar; BIF, breadth of the incisive foramen; BM1, breadth of first upper molar; BMF, breadth of the mesopterygoid fossa; BR, breadth of the rostrum; BZP, breadth of the zygomatic plate; CLM1–3, crown length of the maxillary molar row; HBC, height of the braincase; IB, least interorbital breadth; LB, length of auditory bulla; LBP, length of bony palate; LD, length of the diastema; LIF, length of the incisive foramen; LR, length of the rostrum; ONL, occipitonasal length; PPL, postpalatal length; ZB, greatest zygomatic breadth.

record of the island of Morotai, to the immediate north of Halmahera (K.P. Aplin and K.M. Helgen, unpubl. data).

Distribution: Central Halmahera (see details below under *H. bokimekot* sp. nov.)

Family muridae
Halmaheramys bokimekot Fabre, Pagès, Musser, Fitriana, Semiadi & Helgen gen. et sp. nov.

Types: Holotype: MZB 33266, adult male captured on 15 February 2010. The specimen consists of a dried skin and a cleaned skull (frozen tissue stored in the MZB and Montpellier 2 University DNA collections). The dentition is fully erupted, the skull sutures are fully fused, and the testes are scrotal. External measurements (in mm): head–body 150, tail 132, hind foot 30, ear 19, weight 81 g.

Type locality: The type specimen was collected 15 km north-west of Sagea village, (central Halmahera, Halmahera Island, North Moluccas, Indonesia), at 723 m a.s.l. Coordinates: 00°36′42.60″ N, 128°2′49.00″E.

Paratypes: In addition to the holotype, five specimens of *H. bokimekot* gen. et sp. nov. were collected 11–15 February 2010 at the type locality. All available specimens of *H. bokimekot* gen. et sp. nov. are adult; the description of juvenile traits will have to await the capture of additional specimens.

Etymology: We name the species after the type locality, Boki Mekot, situated in the northern part of Weda Bay, to the north of Sagea village (00°36′42.60″ N, 128°2′49.00″ E). This mountainous area is facing environmental threats from mining and logging operations. By naming the new species after the type locality, we highlight the importance of this

Table 7. Results of principal component analyses comparing *Halmaheramys bokimekot* **gen. et sp. nov.** with seven species of *Taeromys* and *Paruromys dominator*

Variable	Correlations (loadings)			
	Halmaheramys and species of *Taeromys*		*Halmaheramys* and *Paruromys dominator*	
	PC1	PC2	PC1	PC2
ONL	0.97***	0.11	0.99***	−0.05
ZB	0.94***	0.07	0.95***	0.24***
IB	0.57***	0.03	0.60***	0.22***
LR	0.56***	0.43***	0.90***	−0.25***
BR	0.91***	−0.19	0.88***	0.00
BBC	0.90***	−0.07	0.85***	0.34***
HBC	0.71***	−0.13	0.68***	0.22***
BZP	0.77***	0.52***	0.81***	0.21***
LD	0.94***	−0.04	0.90***	−0.20***
PPL	0.92***	−0.13	0.92***	−0.18**
LBP	0.87***	0.17	0.88***	0.21***
BBPM1	0.56***	−0.63***	0.51***	−0.05
BMF	0.43***	−0.75***	0.15**	−0.22***
LIF	0.71***	0.12	0.50***	−0.36***
BIF	0.73***	−0.12	0.54***	−0.19**
LB	0.83***	−0.30**	0.73***	0.04
CLM1–3	0.72***	0.55***	0.77***	0.20***
BM1	0.74***	0.23*	0.65***	0.27***
Eigenvalue	0.111	0.028	0.079	0.010
% Variance	59.8	14.9	66.1	8.2

Correlations (loadings) of 16 cranial and two dental log-transformed variables are based on 351 specimens representing nine species; see Figure 6. *** $P \leq 0.001$; ** $P \leq 0.01$; * $P \leq 0.05$. Abbreviations: BBC, breadth of the braincase; BBPM1, breadth of the bony plate at first molar; BIF, breadth of the incisive foramen; BM1, breadth of first upper molar; BMF, breadth of the mesopterygoid fossa; BR, breadth of the rostrum; BZP, breadth of the zygomatic plate; CLM1–3, crown length of the maxillary molar row; HBC, height of the braincase; IB, least interorbital breadth; LB, length of auditory bulla; LBP, length of bony palate; LD, length of the diastema; LIF, length of the incisive foramen; LR, length of the rostrum; ONL, occipitonasal length; PPL, postpalatal length; ZB, greatest zygomatic breadth.

limestone-rich area for conserving Halmaheran endemic biodiversity.

Vernacular names: We provide vernacular names for *H. bokimekot* gen. et sp. nov., both in English (Spiny Boki Mekot Rat) and in Bahasa Indonesia (Tikus Duri Boki Mekot).

Diagnosis: As for the genus.

Description: Halmaheramys bokimekot gen. et sp. nov. is a terrestrial, spiny rat, of medium body size with brownish grey dorsal fur, greyish white ventral coat, and a short tail (Fig. 7). The head and body are covered by long, harsh and thick fur. The fur is scattered with spiny and bristly hairs. The bristly pelage is primarily located on the dorsolateral part of the back. These hairs are longer in this part of the body, and they have white tips (ranging between one-third white and two-thirds dark and two-thirds white and one-third dark). The tips of the most robust hairs are prolonged into a long, flexible, hair-like structure. The spiny pelage is stiff and flattened, has its most robust guard hairs petiolate, is whitish–grey, and the tip forms a sharp abruptly narrowing point. These hairs are mainly located on the venter, and are scattered on the dorsum of the animal. The colour is nearly uniform on the venter, but slightly patchy on the dorsal part. The upper part of the back from the head to the back is primarily dark brown with some chestnut and brownish greyish hair on the lateral side of the upper part of the legs. The colour on both sides of the body is formed by the overfur. The underfur is short and thick, grey on the dorsum and greyish–whitish ventrally. The hairs of the rump and back are 15–25 mm long, and the coat is dense over the entire body and slightly harsh to the touch. Among the six specimens examined, we did not detect

Figure 7. Colour drawing of ***Halmaheramys bokimekot*** **gen. et sp. nov.** Watercolour by Jon Fjeldså.

any significant variation in colour or texture of the pelage.

Mystacial, submental, supercilliary, genal, and interramal vibrissae ornament the head of *H. bokimekot* gen. et sp. nov. The mystacial, subocular, and supercilliary are long (e.g. 3–4 cm for mystacial). The submental, interramal, and most mystacial vibrissae are not pigmented, and the other vibrissae are blackish. The eyelids are blackish, the ears are brownish grey, and covered both outside and inside by very short and soft hairs.

The two adult females have three pairs of teats: one postaxillary and two inguinal ($0 + 1 + 2 = 6$).

The tail in *H. bokimekot* gen. et sp. nov. is shorter than the head–body length (TL/HB = 81%; Figs 5, 7; Table 1). It is brown on all surfaces except for the distal 5–12 mm, which is white (in five specimens; one lacked the distal part of the tail). Brown overlapping annuli of squarish epidermal scales and brown scale hairs provide the pigmentation for all surfaces of the tail except for the white tip, in which the scales and hairs are unpigmented. Three hairs emerge from beneath each scale, each about as long as a single scale or slightly longer (there are 9–11 scale rings per

cm, as measured near the base of the tail). The unpigmented hairs covering the white tip are longer on average, each covering two scales.

The front and hind feet of *H. bokimekot* gen. et sp. nov. are long and slender. The digits and most of the dorsal surfaces of the front and hind feet are white (covered by short whitish hairs); the inside part of the hind feet displays a fine brownish grey line that extends from ankle to body fur. The sharp and moderately long claws are unpigmented (ivory coloured), and are partly covered by silvery ungual tufts. On the front feet there is a rounded reduced pollex that bears a prominent nail. Palmar and plantar surfaces are naked and unpigmented. Three prominent interdigital mounds along with a large thenar pad and slightly smaller hypothenar adorn the palmar surface. Four interdigital mounds, one small hypothenar, and an elongate thenar comprise the pad topography on the plantar surface.

Views of the skull of *H. bokimekot* gen. et sp. nov. are shown in Figure 8. The braincase is smoothly vaulted, the interorbit moderately broad, low and inconspicuous beading outlines the dorsolateral margins of the interorbital and postorbital regions,
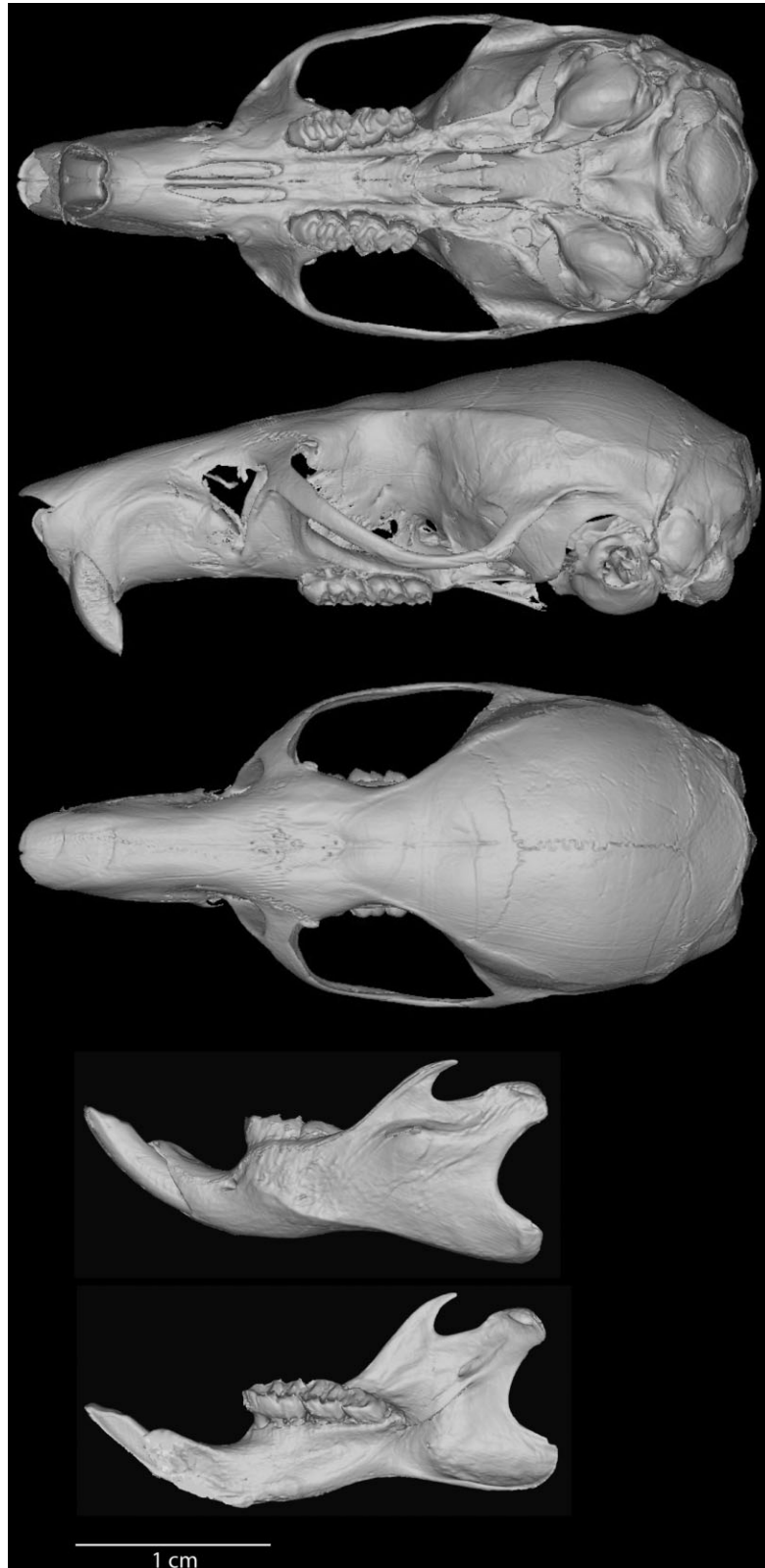
Figure 8. Skull of ***Halmaheramys bokimekot* gen. et sp. nov.** (holotype MZB 33266) from Boki Mekot (Halmahera, Indonesia), shown in palatal (top), left lateral (2nd line), and dorsal (third line) views of crania, lateral views of left mandibles (fourth line), and medial views of right mandible (bottom).

and the rostrum is moderately long and narrow. On each side of the rostrum, the lacrymal capsule is slightly inflated. From the dorsal view, the rostrum appears rounded at the distal end because of the nasal bone, which curves slightly downwards dorsoventrally. The zygomatic plate curves forwards forming a shallow notch between the plate and the side of the rostrum. The interorbital region is broad; two small mounds are formed by the frontal bones. Dorsolateral margins of the interorbital and postorbital regions are linked with the smooth dorsolateral margin of the braincase by low ridges. The oblique lambdoid crest is slightly smooth and truncates the smooth posterior sweep of the braincase. The interparietal forms a roof over most of the moderately deep occipital region. The sides of the braincase are vertical from the squamosal roots of the zygomatic arches to the temporal beading. The thin zygomatic arch curves slightly away from the outline of the braincase at an angle near to the zygomatic plate, from which the zygomatic arch originates.

In ventral view, the narrow bony palate (scored by a pair of palatine grooves) extends to the back margins of the third molars. The small posterior palatine foramina pierce the bony palate at the level where second and third upper molars touch. Tooth rows are not parallel, diverging posteriorly. The incisive foramina are moderately wide and long (relative to the length of the rostrum), extending posteriorly to the alveolar margins of the first upper molars. The distal margins of the nasals and premaxillary form a short extension beyond the anterior faces of the incisors. The posterior one-third of the maxillary root of the zygomatic plate is located at the level of the first upper molars. The mesopterygoid fossa is slightly narrower than the bony palate, and its anterodorsal walls are breached by short sphenopalatine vacuities. The pterygoid regions are long and developed. There is a sphenopterygoid vacuity that is open on each pterygoid plate. There is a ridge along the lateral margin of each pterygoid plate that converges posteriorly and posterolaterally behind the foramen ovale opening, and forms the anterior border of the medial lacerate foramen. The auditory bullae are very small in relation to the size of the cranium. The eustachian tubes are short and narrow. As in *Bunomys prolatus* Musser, 1991, the medial sagittal plane of the bullar capsule is oriented ventromedially (see Musser, 1991). The posterior margin of the occiput overhangs the occipital condyles.

The rostrum, auditory bullae, interorbit, and top of the parietal can be seen in side view (Fig. 8). As illustrated in Figure 8, the tip of the nasal and the distal parts of the premaxilla project anterior to the incisors. The rostrum is high relative to its length and width. The zygomatic arches do not significantly extend outwards from the braincase. The zygomatic plate curves dorsally from the maxillar base, has a trapezoidal shape between the upper part of the zygomatic arch and the proximal part of the maxillary root until the ventral part of the zygomatic plate. The maxillary root of the zygomatic plate originates at the level of the first upper molar. The zygomatic plate is narrow, and the anterior edge is convex. The nasolacrimal foramen displays an opening in front of the zygomatic plate within the nasolacrimar capsule. The squamosal root of the zygomatic arch is relatively low on the side of the skull, and its posterior margin curves from the postglenoid fossa to the occiput. The mastoid portion of the periotic is slightly extended without any vacuity. The squamosal bone near the auditory bullae is complete (no squamosomastoid foramen). The middle lacerate foramen is wide and links ventrally to the wide postglenoid foramen. The anterior opening of the alisphenoid canal and foramen ovale open on the lateral side of the skull in front of the postglenoid vacuity area, below the squamosal root of the zygomatic arch. The alisphenoid canal is found below the squamosal part of the zygomatic root and above the margin of the pterygoid crest. An alisphonoid strut is absent (see Musser & Newcomb, 1983). The pterygoid plates are clearly visible, with a developed hamular process.

All six specimens of *H. bokimekot* gen. et sp. nov. possess a carotid arterial circulation that is considered as a derived character for muroid rodents generally, but as primitive for the subfamily Murinae (character state 2 of Carleton, 1980; pattern 2 described by Voss, 1988; conformation illustrated for *Oligoryzomys* by Carleton & Musser, 1989), and common among murines (Musser & Newcomb, 1983; Musser & Heaney, 1992). The pattern is reflected in certain cranial foramina and bony landmarks in cleaned skulls, as well as in dried blood vessels left on incompletely cleaned skulls. No sphenofrontal foramen penetrates the bony junction of the orbitosphenoid, alisphenoid, and frontal bones; no squamosal–alisphenoid groove scores the inner surface of each wall of the braincase; and no shallow trough extends diagonally over the dorsal (inner) surface of each pterygoid plate. There is a large stapedial foramen in the petromastoid fissure, and a deep groove extending from the middle lacerate foramen to the foramen ovale on the ventral posterolateral surface of each pterygoid plate. This disposition of foramina and grooves indicates that the stapedial artery branches from the common carotid, enters the periotic region through a large stapedial foramen, and that the infraorbital artery exits the periotic through the middle lacerate foramen, then courses in a short groove on the outside of the pterygoid plate, to disappear into the braincase through the alisphenoid canal, from which it emerges

MZB 33266   MZB 33265   MZB 33263   MZB 33264

Figure 9. Occlusal views of the right maxillary upper molar rows. From left to right: holotype of adult ***Halmaheramys bokimekot* gen. et sp. nov.** (MZB 33266, crown length of the maxillary molar row, CLM1–3, 6.51 mm); Paratypes of ***H. bokimekot* gen. et sp. nov.** (MZB 33265, CLM1–3 = 6.77 mm; MZB 33263, CLM1–3 = 6.66 mm; MZB 33264, CLM1–3 = 6.74 mm).

to course through the anterior alar fissure into the orbit. The supraorbital branch of the stapedial is absent.

Each dentary is stocky (Fig. 8), with a short and thick region between the incisor alveolus and molar row. The prominent coronoid process is separated by a deep sigmoid notch from the broad condylar process. The angular process is short and wide, forming a moderately deep concavity with the condylar process, which together form the posterior margin of the dentary. There is a developed masseteric ridge extending from below the first lower molar to the lower end of the wide angular process. Each incisor is contained within an alveolar capsule, which is expressed on the lateral surface of the dentary by a moderate bulge beneath the coronoid process. There is a low ridge forming a slight connection with the molar platform of the condyle. Along this ridge and below the back of the condyle is the opening of the mandibular foramen.

The upper and lower incisors of *H. bokimekot-* gen. et sp. nov. are broad, and their enamel is orange. The upper incisors are orthodont, projecting from the rostrum at a right angle in all six specimens examined. The molars of *H. bokimekot* gen. et sp. nov. have multiple roots, which were identified with a µCT scanner. Below each first upper molar, we found one large anterior root, two smaller lingual anchors, one labial root, and one large posterior root. Four roots anchor each second molar; there are two anterior

roots and a posterior anchor below each third molar. One anterior and one posterior root coupled with smaller labial and lingual anchors attach to each first lower molar. The second and third lower molars are both anchored by two anterior and one posterior roots. The alveoli patterns of upper and lower molar roots seen in *H. bokimekot* gen. et sp. nov. are similar to the patterns depicted for *B. prolatus* (see Musser, 1991).

The molars are elongate and brachyodont (Figs 9, 10). Because of the lack of the anterocone/id, the second molar is smaller than the first molar, and the third molar is half the size of the second molar. The first upper molar overlaps the upper second molar, and the upper second molar overlaps the upper third molar. Within the mandibular rows, the third molar inclines on the second molar around the postero-cingulum cusp, and the second molar slightly overlaps the first molar. With respect to the occlusal pattern of the upper molars, the lamina on the upper molar rows are obliquely orientated in a anteroposterior plan, giving an elongated shape to the teeth. Cusp t3 of each upper molar is completely fused with the central cusp t2, forming a lamina. This lamina is caudally projected on the labial side between cusps t2 and t1, which are nearly fused. A second lamina is formed via linking cusps t4, t5, and t6. The lingual margin of the first upper molar is formed by cusps t1, t4, and t8. The anterolabial margins of the second and third upper molars lack cusp t3 (see Musser &
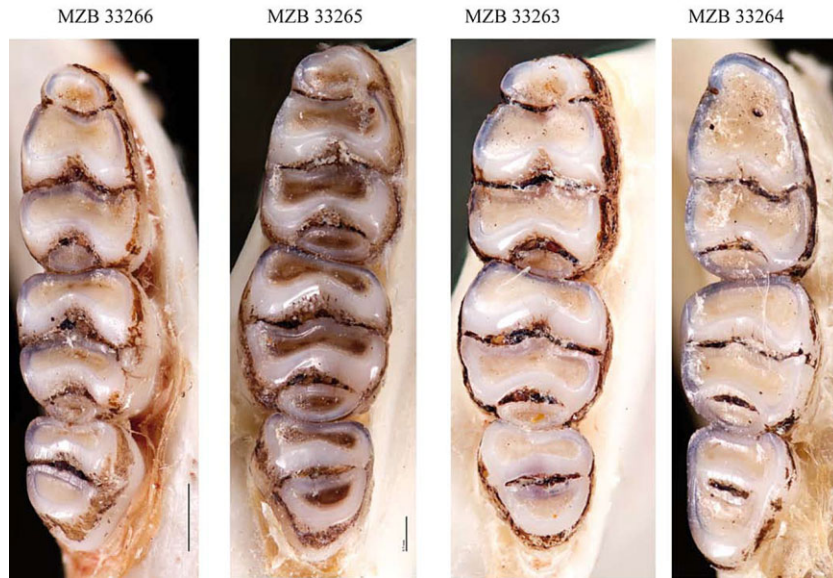
Figure 10. Occlusal views of lower molar rows. From left to right: holotype of ***Halmaheramys bokimekot* gen. et sp. nov.** (MZB 33266, crown length of the maxillary molar row, CLM1–3, 6.42 mm); paratypes of ***H. bokimekot* gen. et sp. nov.** (MZB 33265, CLM1–3 = 6.46 mm; MZB 33263, CLM1–3 = 6.30 mm; MZB 33264, CLM1–3 = 6.54 mm).

Newcomb, 1983 for diagrams and terminology of cusps and cusplets).

On the third upper molar, cusp t1 stands separate from row t4, t5, and t6, even in well-worn teeth. The C-shaped lamina – formed by the tight fusion of cusps t4, t5, and t6 – is also separate from the posterior lamina (consisting of cusp t8; if cusp t9 is also present it is undetectable) and is only connected in worn teeth.

Occlusal patterns formed by cusps of the lower molars are also simple (Fig. 8). The laminae of the lower molar rows are obliquely orientated in a postero-anterior way. Two specimens showed posterior labial cusplets on the first and second molars. The occlusal pattern of the first lower molar consists anteroposteriorly of: (1) an oblong lamina, formed by the fusion of a large anterolingual cusp and a smaller anterolabial cusp; (2) a wide second lamina that links the lingual metaconid to the labial protoconid; (3) a wide third lamina, encompassing the lingual entoconid and the labial hypoconid, can be linked to a small posterior labial cusplet, observed in two specimens; (4) a well-developed posterior cingulum. The second lower molar lacks the anterolabial and anterolingual cuspids, but displays the same patterns among the lamina as in the first upper molar. The laminae linking the protoconid/metaconid and hypoconid/entoconid are both wide along their anteroposterior axis, and form the shape of an 'M'. The labial cuspids are also more developed than the lingual ones. A small posterolabial cusplet occurs on two specimens (MZB 33266 and 33264) on the first and second lower

molars. The third lower molar is smaller than the second. The occlusal surface consists of two large laminae. The front lamina is formed by the protoconid and metaconid, and the posterior lamina is formed by the fusion of the entoconid and hypoconid. A posterior cingulum is absent, and there are no posterior or anterolabial cusplets.

We also provided cytochrome *c* oxidase I (*COI*; KF164277) for DNA barcoding purposes. We used *COI* primers BatL5310 (5′-CCTACTCRGCCATTTTACCT ATG-3′) and R6036R (5′-ACTTCTGGGTGTCCAAA GAATCA 3′) with the protocol described by Robins *et al*. (2007).

Comparisons: A monophyletic clade containing the Sundaic *Sundamys*, Philippine *Bullimus*, Sulawesian *Bunomys*, *Taeromys*, and *Paruromys*. and Moluccan *Halmaheramys* was recovered from our molecular analyses (clade G in Fig. 2). Within this cluster, *Halmaheramys* gen. nov. was sister to the Sulawesian clade comprised of *Bunomys*, *Taeromys*, and *Paruromys* (clade H in Fig. 2). Consequently, we concentrate most attention on comparisons of *Halmaheramys* gen. nov. with three genera. The diagnosic traits for *Halmaheramys* gen. nov. are sufficient for it to be recognized as an unique taxonomic entity, generically distinct from the Sulawesian *Bunomys*, *Taeromys*, and *Paruromys*. We also provide summaries of qualitative morphological distinctions between *Halmaheramys* gen. nov. and other Sundaic and Philippine genera.

Halmaheramys and Bunomys: In its moderate body size and relatively short tail, *H. bokimekot* gen. et sp. nov. recalls species of *Bunomys*, especially *B. chrysocomus*, but the resemblance is superficial. Compared with species of *Bunomys*, the Halmahera rat is smaller, has a much shorter tail and hind feet, and smaller ears (Table 1). Its fur is harsh and bristly (dense and soft in all species of *Bunomys*), tail scales are large (much smaller in *Bunomys*), and females have three pairs of teats (all *Bunomys* have two pairs, both inguinal).

The cranial conformations of *H. bokimekot* gen. et sp. nov. and *B. chrysocomus* (in body size the smallest of the *Bunomys*) are remarkably similar, and prompted us to initially identify the Halmahera animal as a species of *Bunomys* (most similar to *B. chrysocomus*; see images of skulls of various species of *Bunomys* in Musser, 1991). However, details of size and proportion exclude the Halmaheran taxon from *Bunomys*. Occipitonasal length, interorbital breadth, length of rostrum, breadth of zygomatic plate, and breadth of upper molars are similar in the two species, as judged by mean values for these dimensions, but nearly all other cranial dimensions in *H. bokimekot* gen. et sp. nov. are on average smaller; height of braincase, breadth of mesopterygoid fossa, and length of maxillary tooth row are the exceptions, being greater in *H. bokimekot* gen. et sp. nov. (Table 3).

Cranial and dental similarities and distinctions, as indicated by univariate statistics and visual inspection of skulls, are summarized in the two graphs in Figure 5, where the distribution of specimen scores are projected on the first and second components extracted from a principal components analysis. In the upper graph, covariation among most variables indicated size to be the primary factor dispersing scores along the first component, as shown by positive, high correlations on this axis ($r = 0.50$–0.93; Table 6). Species with smaller skulls are plotted more to the left, and those with larger skulls are plotted to the right. Scores for the six examples of *H. bokimekot* gen. et sp. nov. are contained within the large cloud of points representing the sample of *B. chrysocomus*. *Halmaheramys bokimekot* gen. et sp. nov. and *B. chrysocomus* are similar in absolute cranial dimensions, contrasting with the other species of *Bunomys* with larger skulls (Table 3).

Covariation among variables on the second component reflected similarities and differences in the proportions of cranial and dental measurements, and here again *H. bokimekot* gen. et sp. nov. was indistinguishable from *B. chrysocomus*, at least in the context in which all species of *Bunomys* were included in the analysis.

Finer resolution distinctions are summarized in the lower graph in Figure 5, where scores for *H. bokimekot* gen. et sp. nov. and *B. chrysocomus* form two discrete clusters along the second axis, reflecting proportional distinctions between the species. Covariation among particular variables, as indicated by moderate to high loadings in Table 6, is responsible for the separation of scores into these two non-overlapping constellations. Compared with *B. chrysocomus*, *H. bokimekot* gen. et sp. nov. (Fig. 5; Table 6) has a relatively narrower zygomatic breadth, braincase, and bony palate ($r = 0.26$, 0.18, and 0.30), wider zygomatic plate and mesopterygoid fossa ($r = -0.21$ and -0.82), shorter diastema, bony palate, and incisive foramina ($r = 0.32$, 0.22, and 0.37), smaller bullae ($r = 0.55$), and longer maxillary molar row ($r = -0.18$).

Although occlusal patterns of cusps on the molars are similar in *H. bokimekot* gen. et sp. nov. and *B. chrysocomus*, they differ in several aspects. In *H. bokimekot* gen. et sp. nov., the molars are narrower, the anteroconid is formed of large anterolingual and anterolabial cusps, broadly fused into a single lamina that is elliptical or oblong in cross section (versus retaining the cuspidate configuration in *B. chrysocomus*), the anterolabial cusp is not present on second and third lower molars (typically present in *B. chrysocomus*; see the images in Musser & Newcomb, 1983: 399), and the anterior labial cusplets are not evident on the first and second lower molars (present in about half of any large sample of *Bunomys*; see Table 8).

Halmaheramys and Taeromys: Taeromys comprises species of relatively large body size with tails typically equal to or longer than length of head and body, a physical conformation that contrasts with *H. bokimekot* gen. et sp. nov., which is diminutive in body size and short-tailed (Table 1). Species of *Taeromys* typically have: short, soft, and dense fur composed of thin and pliable hairs (harsh and bristly in *H. bokimekot* gen. et sp. nov.); a bicolored tail in which the basal one-third to one-half is dark brown, and the distal segment white (only a short white tip in *H. bokimekot* gen. et sp. nov.); smooth, glistening tail surfaces because of non-overlapping rings of thin scales and very short, fine-scale hairs (overlapping annuli of large scales so tail surface appears ragged rather than smooth in *H. bokimekot* gen. et sp. nov.); and either three pairs of mammae (one postaxillary pair and two inguinal pairs) or two inguinal pairs only (one postaxillary and two inguinal pairs in *H. bokimekot* gen. et sp. nov.).

The disparity in physical size between the species of *Taeromys* and *H. bokimekot* gen. et sp. nov. is paralleled by the stark contrasts in cranial and dental measurements (Table 5). A large robust skull with broadly flaring zygomatic arches, a long rostrum, and wide zygomatic plates is typical of *Taeromys* (see

Table 8. Configuration of cusp t4 on M1 and M2 (applies only to *Paruromys dominator*) and presence (+) or absence (−) of particular cusps on maxillary (M1–3) and mandibular (m1–3) molars in samples from species of ***Halmaheramys bokimekot* gen. et sp. nov.**, *Bunomys*, *Taeromys*, and *Paruromys*. Number of cusps and cusplets are expressed as percentages; number of specimens are in parentheses

	Halmaheramys gen. nov.	*Bunomys*	*Taeromys*			*Paruromys*
	H. bokimekot gen. et sp. nov.	*B. chrysocomus*	*T. celebensis*	*T. callitrichus*	*T. hamatus*	*P. dominator*
MAXILLARY MOLARS						
Cusp t4						
M1						
Divided or bilobate	−	−	−	−	−	70 (204)
Whole	−	−	−	−	−	30 (89)
M2						
Divided or bilobate	−	−	−	−	−	85 (250)
Whole	−	−	−	−	−	15 (43)
Cusp t3						
M2						
+	−	17 (33)	98 (59)	100 (5)	73 (11)	99 (294)
−	100 (6)	83 (164)	2 (1)	−	27 (4)	4 (1)
M3						
+	−	5 (10)	85 (51)	−	53 (8)	85 (250)
−	100 (6)	95 (187)	15 (9)	100 (5)	47 (7)	15 (43)
MANDIBULAR MOLARS						
m1						
Anterior labial cusplet						
+	−	52 (62)	23 (13)	−	13 (2)	66 (207)
−	100 (6)	48 (58)	78 (43)	100 (5)	87 (13)	34 (109)
Posterior labial cusplet						
+	33 (2)	97 (116)	100 (58)	100 (5)	73 (11)	100 (316)
−	67 (4)	3 (4)	−	−	27 (4)	−
m2						
Anterolabial cusp						
+	−	90 (108)	98 (54)	100 (5)	100 (15)	99 (314)
−	100 (6)	10 (12)	2 (1)	−	−	1 (2)
Posterior labial cusplet						
+	33 (2)	98 (117)	100 (57)	100 (5)	27 (4)	100 (316)
−	67 (4)	2 (3)	−	−	73 (11)	−
m3						
Anterolabial cusp						
+	−	65 (78)	57 (24)	−	93 (14)	96 (303)
−	100 (6)	35 (42)	43 (22)	100 (5)	7 (1)	4 (13)

the cranial images in Musser & Newcomb, 1983); by comparison, the skull of *H. bokimekot* gen. et sp. nov. is gracile and small. Distinctions in size and proportions are summarized in the upper graph in Figure 2, where specimen scores are projected on the first and second components extracted from principal components analysis. Along the first axis covariation among all variables, as indicated by moderate to large loadings ($r = 0.43$–0.97; Table 7), point to size as being responsible for the distribution of scores into a cluster identifying *H. bokimekot* gen. et sp. nov. in the left half of the ordination, with the scores representing the seven species of *Taeromys* aligned in the right half. This is not surprising, and simple visual observation of skulls and toothrows reveals the same magnitude of size disparity.

The alignment of scores along the second component reflects proportional distinctions for some variables not so easily recognized with side-by-side inspection of skulls. Compared with the species of *Taeromys* (Fig. 6; Table 7), the Halmahera rat has a relatively shorter rostrum and molar row ($r = 0.43$

and 0.55, respectively), narrower zygomatic plate ($r = 0.52$), wider bony palate and mesopterygoid fossa ($r = -0.63$ and -0.75, respectively), larger bulla ($r = -0.30$), and narrower first molar ($r = 0.23$).

There are some dental contrasts between the two genera. The molars of *Taeromys* typically have higher crowns than those of *H. bokimekot* gen. et sp. nov., cusp t3 is usually present on the second and third upper molars (absent in *H. bokimekot* gen. et sp. nov.), the anteroconid is formed of fused large anterolingual and anterolabial cusps that retain its bicuspidate nature (broadly fused into a single lamina that is elliptical or oblong in cross section in *H. bokimekot* gen. et sp. nov.), and anterolabial cusps are present on second molars in all species and on the third lower molars in most but not all of the species (absent from both molars in *H. bokimekot* gen. et sp. nov.; see Table 8 and the images of toothrows for *Taeromys* in Musser & Newcomb, 1983: 492–493).

Halmaheramys and Paruromys: The largest Sulawesian Murine, *P. dominator*, which has both arboreal and terrestrial habits, is a giant compared with the much smaller and terrestrial *H. bokimekot* gen. et sp. nov. (Tables 1, 5). Also, compared with *H. bokimekot* gen. et sp. nov., the larger-bodied *Paruromys* has a much longer tail relative to the head–body length, soft and dense fur, small epidermal tail scales, and a bicolored tail that is similar in patterning to tails of the species of *Taeromys*.

The large elongate and robust skull of *P. dominator*, with its widely flaring zygomatic arches, wide zygomatic plate, short incisive foramina terminating well anterior to front margins of the first molars, and long bony palate extending far enough past posterior margins of the third molars to form a narrow shelf, is an appreciable contrast to the much smaller and gracile skull of *H. bokimekot* gen. et sp. nov. (see the cranial images for *P. dominator* in Musser & Newcomb, 1983). In fact, it shows only a slight flare to the zygomatic arches, narrow zygomatic plates, longer incisive foramina that reach anterior borders of first molars, and a shorter bony palate that does not extend beyond the third molars. These distinctions are readily evident when skulls of each species are visually examined side-by-side. Multivariate analysis of cranial and dental measurements reinforces these visual contrasts, and also provides a summary of proportional differences in some variables. In the lower graph in Figure 6, specimen scores are projected on the first and second principal components extracted from principal components analysis. Along the first axis, covariation among all variables, as indicated by the moderate to large correlations ($r = 0.50$–0.99; Table 6), identify size as responsible for spreading the specimen scores into two widely separated clusters: scores for *H. bokimekot* gen. et sp. nov. in the left half of the graph and scores representing *P. dominator* in the right half. The pattern is similar to that seen in the principal components ordination contrasting *Halmaheramys* with species of *Taeromys* (upper graph in Fig. 6).

Covariation among most variables on the second component, as indicated by the significant positive and negative loadings listed in Table 7, and the spread of specimen scores along the second axis – with the cluster for *H. bokimekot* gen. et sp. nov. lower in the graph compared with most scores representing *P. dominator* – quantitatively summarize the proportional distinctions between the two species, in particular in cranial and dental variables. Compared with *P. dominator*, the Halmahera species is relatively narrower across the zygomatic arches (a reflection of the slight bow in the arches), has a relatively narrower interorbital region and zygomatic plate, smaller braincase, shorter bony palate, and smaller molars (shorter molar row and narrower molars); but has a relatively longer rostrum, diastema, and postpalatal region, wider mesopterygoid fossa, and longer and wider incisive foramina. The skull of *H. bokimekot* gen. et sp. nov. is not just a smaller version of *P. dominator* but is also proportionally different.

The molars of *H. bokimekot* gen. et sp. nov., in addition to being absolutely and relatively smaller than those in *P. dominator*, also differ in molar occlusal patterns (compare the images of molars for *H. bokimekot* gen. et sp. nov. in Figs 9 and 10, with those for *P. dominator* in Musser & Newcomb, 1983: 508–509). Cusp t4 on first and second maxillary molars is entire (not divided into cusps or bilobed) in all specimens of *H. bokimekot* gen. et sp. nov., but comparable cusps are divided into two cusps or bilobed in three-quarters or more of any large sample of *P. dominator* (Table 8), cusp t3 is absent from second and third upper molars (typically present in *P. dominator*), the anteroconid is formed of fused large anterolingual and anterolabial cusps that form a single lamina, elliptical or oblong in cross section (retains its bicuspidate nature in *P. dominator*), anterolabial cusps are not evident on the second and third lower molars (typically present in *P. dominator*), anterior labial cusplets are not present (occurring in about three-quarters of the sample of *P. dominator*), and posterior labial cusplets are found in only two of the six specimens (typically present in *P. dominator*); see Table 8.

Beyond its close relationship with Rattini genera from Sulawesi, *Halmaheramys* is phylogenetically most closely related to Sundaic *Sundamys* and Philippine *Bullimus*, as estimated by analyses of DNA sequences (clade G in Fig. 2). *Sundamys muelleri* (Jentink, 1879), *Sundamys infraluteus* (Thomas,

1888), and *Sundamys maxi* (Sody, 1932) are the currently recognized species in *Sundamys* (Musser & Newcomb, 1983; Musser & Carleton, 2005); *Bullimus luzonicus* (Thomas, 1895), *Bullimus bagobus* (Mearns, 1905), and *Bullimus gamay* (Rickart, Heaney & Tabaranza, 2002) comprise *Bullimus* (Rickart, Heaney & Tabaranza, 2002). Although morphological traits enumerated in the diagnosis of *Halmaheramys* serve to distinguish that genus from *Sundamys* and *Bullimus*, we briefly highlight here particular morphological differences between the Halmaheran endemic and these Sundaic and Philippine clusters of species.

Differences in body size, tail patterning, and number of teats constitute the most apparent distinctions between the Halmahera endemic and the other two genera. Compared with *H. bokimekot* gen. et sp. nov., all the species of *Sundamys* and *Bullimus* are much larger rats (Table 9), comparable in body size to *P. dominator* and the larger-bodied species of *Taeromys* (Table 1). The tail is monocoloured brown and appreciably longer than the head–body length in all species of *Sundamys* (TL/HB = 119–122%), whereas the tail is shorter than the head–body length in *Bullimus* (TL/HB = 76–84%), with a proportion similar to that in *H. bokimekot* gen. et sp. nov. (TL/HB = 79–85%), it is brown over the basal one-third or half, and white for the rest of the tail (see fig. 5 in Rickart *et al.*, 2002: 429), whereas *H. bokimekot* gen. et sp. nov. has a brown tail with a short white tip. Two of the three species of *Sundamys* have four pairs of teats (one pectoral, one postaxillary, and two inguinal), all *Bullimus* also show four pairs of teats, but the distribution on the body is different (one postaxillary, one abdominal, and two inguinal), and one postaxillary and two inguinal pairs are found in *H. bokimekot* gen. et sp. nov. Additional external distinctions can be detected by comparing our description of *H. bokimekot* gen. et sp. nov. with the detailed expositions of *Sundamys* presented by Musser & Newcomb (1983), and of *Bullimus* by Musser & Heaney (1992) and Rickart *et al.* (2002).

Skulls of all species of *Sundamys* and *Bullimus* are large compared with that of the much smaller *H. bokimekot* gen. et sp. nov. (Table 9), and are robust in overall conformation, in opposition to the elongate and gracile skull of the Halmaheran endemic (compare the images of *H. bokimekot* gen. et sp. nov. in Figure 8 with those of *Sundamys* shown by Musser & Newcomb, (1983) and *Bullimus* portrayed in Musser & Heaney (1992) and Rickart *et al.* (2002)). The cranial stockiness of *Sundamys* and *Bullimus* is accentuated by their strong, widely flaring zygomatic arches and broad zygomatic plates (with associated deep zygomatic notches), both presenting a striking contrast to the weakly bowed arches of *H. bokimekot*

gen. et sp. nov. and its very narrow zygomatic plates (and barely perceptible zygomatic notches). Most specimens of *Sundamys* exhibit an alisphenoid strut (see Musser & Newcomb, 1983: 416; table 15), but a comparable structure is not found in *H. bokimekot* gen. et sp. nov., and the Javan *S. maxi* possesses a derived carotid arterial circulation unlike the primitive pattern (for murines) seen in the Halmaheran genus. Each ectotympanic bulla of *Bullimus* is inflated and large relative to the size of the skull, and its configuration is unique among Asian murines: the external auditory meatus is oriented posteriorly and bounded medially by an expansive posterior lamina, and laterally by a bony shield, as described and illustrated by Musser & Heaney (1992: 118; fig. 75); the ectotympanic capsule of *H. bokimekot* gen. et sp. nov. is small relative to the size of the skull, and its configuration resembles that of *Rattus* and most other Asian murines, as exemplified by the images of *R. everetti* presented in Musser & Heaney (1992: 118).

Paralleling the larger skulls of *Sundamys* and *Bullimus* are their larger molars, as compared with the smaller teeth of *Halmaheramys*, and there are other differences. Molar occlusal patterns in *Sundamys* are slightly more complex in that a posterior cingulum is present on the first upper molar in *S. infraluteus* and *S. maxi*, and half of any large sample of *S. muelleri* (not present in *H. bokimekot* gen. et sp. nov.), cusp t3 is part of the chewing surface of the second and third upper molars (absent from counterparts in *H. bokimekot* gen. et sp. nov.), each second and third lower molar bears an anterolabial cusp (not present in *H. bokimekot* gen. et sp. nov.), anterior labial cusplets are present on the first lower molar in many specimens, and posterior labial cusplets are typically part of the occlusal surfaces of the first and second lower molars (anterior labial cusplets are not evident in the six examples of *H. bokimekot* gen. et sp. nov., and posterior labial cusplets occur infrequently); compare the cusp and cusplet frequencies in Table 8 with those summarized for *Sundamys* in Musser & Newcomb (1983: 421; table 17), and images of molar rows for *H. bokimekot* gen. et sp. nov. in Figures 9 and 10 with those for the species of *Sundamys* provided by Musser & Newcomb (1983).

Species of *Bullimus* have bulky, hypsodont molars, in strong contrast to the smaller brachydont molars in *H. bokimekot* gen. et sp. nov. The two genera are additionally distinguished by the presence of anterolabial cusps on the second and third lower molars in *Bullimus*, and their absence in the Halmahera endemic (compare the images of molar rows for *H. bokimekot* gen. et sp. nov. in Figures 9 and 10 with those for species of *Bullimus* provided by Musser & Heaney, (1992: 120; fig. 76).

Table 9. Descriptive measurements for head–body length (HB), tail length (TL), hind foot (HF), and ear (E), in mm, and for weight in grams (WT), for *Halmaheramys bokimekot* **gen. et sp. nov.**, and for species of *Sundamys* and *Bullimus*

Species	HB	TL	HF	E	WT	TL/HB (%)	ONL
Halmaheramys gen. nov.							
H. bokimekot gen.	153.2 ± 12.33	121.6 ± 1.55	28.1 ± 0.48	18.4 ± 1.12	89.3 ± 15.04	79	38.2 ± 3.64
et sp. nov. ♀	(143.2–167.0) 3	(119.9–122.9) 3	(27.5–28.4) 3	(27.5–28.4) 3	(72–99) 3		(36.9–39.2) 3
H. bokimekot gen.	149.0 ± 2.71	126.0 ± 9.02	29.6 ± 0.49	18.9 ± 0.94	89.7 ± 8.50	85	38.7 ± 3.65
et sp. nov. ♂	(145.9–151.1) 3	(119.6–132.3) 3	(29.2–30.1) 3	(18.1–19.9) 3	(81–98) 3		(38.1–39.2) 3
Sundamys							
S. muelleri	207.3 ± 17.1	260.6 ± 24.6	45.3 ± 2.2	21.4 ± 0.9	–	121	51.1 ± 3.3
(Sumatra)	(185–236) 23	(214–301) 22	(42–49) 23	(20–23) 23			(45.7–58.8) 23
S. infraluteus	258.5 ± 17.5	315.8 ± 18.4	57.5 ± 1.8	24.8 ± 1.6	–	122	60.9 ± 2.1
(Sabah)	(229–282) 10	(289–343) 10	(55–61) 11	(22–27) 10			(55.9–63.3) 13
S. maxi	241.5 ± 16.3	286.7 ± 16.5	53.1 ± 1.0	25.4 ± 1.4	–	119	58.7 ± 2.5
(West Java)	(218–270) 8	(258–309) 7	(52–55) 8	(24–28) 7			(56.3–61.7) 6
Bullimus							
B. luzonicus	247.3 ± 14.4	209.0 ± 21.4	53.6 ± 1.6	32.0 ± 1.4	485.0 ± 49.5	84	55.9 ± 1.0
(Luzon)	(234–267) 4	(2190–233) 4	(51–56) 8	(31–34) 2	(450–520) 2		(54.9–56.8) 3
B. bagobus	250.3 ± 15.6	192.3 ± 5.5	52.3 ± 0.6	27.0 ± 1.7	431.7 ± 18.9	77	61.4 ± 1.7
(Leyte)	(234–265) 3	(186–196) 3	(52–53) 3	(26–29) 3	(410–445) 3		(59.0–64.3) 10
B. gamay	234.5 ± 8.8	177.6 ± 17.7	51.6 ± 2.4	26.0 ± 1.6	367.8 ± 73.6	76	53.0 ± 2.2
(Camiguin)	(223–244) 8	(142–199) 9	(47–54) 9	(23–26) 9	(290–500) 9		(50.8–56.0) 4

Mean ± SD, observed range (in parentheses), and size of sample are provided. Statistics for the samples of *Sundamys* are extracted from Musser & Newcomb (1983); those for *Bullimus* are from Rickart *et al.* (2002). ONL, occipitonasal length.

Natural history: In 2010, the mammalogical team of the MZB trapped six specimens of *H. bokimekot* gen. et sp. nov. in central Halmahera (Fig. 1), at a site located between 700 and 750 m a.s.l., in the southern part of Halmahera Island, north of Weda Bay. The type locality was situated at 723 m a.s.l. Boki Mekot is in a rugged hilly region, with dense primary lowland evergreen forest (Whitmore, 1987) and patches of open, old secondary growth (dominated by trees with small diameter trunks). No large rivers are within 15 km, but a small creek, with a gravel bed and slow, shallow water, remains active during the dry season. The soils have high nickel content, with thin humus (5–10 cm). The closest village is approximately 50 km from the trapping site. This is a mountainous area dominated by limestone and laterite. The surrounding highland rainforest is tall ($\geq$ 30 m) and characterized by the following angiosperm families: Fagaceae (dominated by *Lithocarpus* species), Guttiferacea (nine species), Calophyllacea (dominated by *Calophyllum* species), Lauraceae (seven species dominated by *Litsea* species), and Myrtaceae (11 species dominated by *Eugenia* and *Pometia* species). Gymnosperms (Podocarpaceae), tree ferns, *Ficus*, rattans, bamboo, non-woody climbers, orchids, epiphytes, and bryophytes are also present (Sidiyasa & Tantra, 1984; Whitmore, 1987; Edwards *et al.*, 1990; Flannery, 1995; Monk, Fretes & Reksodiharjo-Lilley, 1997). Specimens of *H. bokimekot* gen. et sp. nov. were captured in folding rat traps placed in runways beneath tree trunks lying on the ground, at burrow openings, and on tree trunks lying on or in subsurface spaces among tree roots. All specimens were trapped in primary forest. The bait consisted of roasted coconut and peanut butter. *Halmaheramys bokimekot* gen. et sp. nov. may be omnivorous, as stomach contents ($n = 2$) contained both vegetable and arthropod remains. Further study is needed in order to characterize the diet of *Halmaheramys*. Specimens collected at the type locality, between 10 and 15 January 2010 included three adult males with scrotal testes, and three adult females, one with an inactive reproductive tract and two with active reproductive tracts (one was pregnant with three embryos). At the type locality, *H. bokimekot* gen. et sp. nov. was trapped in association with *R. exulans*, *R. morotaiensis*, *Phalanger ornatus* (Gray, 1860), *Suncus murinus* (Linnaeus, 1766), and *Viverra tangalunga* (Gray, 1832).

Distribution: Known only from the type locality, Boki Mekot (Fig. 1). We predict that this rat will be found to be more widely distributed in appropriate forested habitats in Halmahera, and perhaps on adjacent islands with close Halmaheran biogeographic associations (e.g. Bacan, Morotai, Ternate, and Tidore).

THE AFFINITIES OF *HALMAHERAMYS* AND SYSTEMATICS OF THE RATTINI

Our phylogenetic analyses (Figs 2 and 3) are in general agreement with those of previous Murinae supermatrices (Steppan *et al.*, 2005; Jansa *et al.*, 2006; Lecompte *et al.*, 2008; Rowe *et al.*, 2008; Heaney *et al.*, 2009). Within the Rattini, we found a divergence between *Micromys minutus* and all other genera in Rattini. Our results also confirmed the polyphyly of the *Micromys* division *sensu* Musser & Carleton (2005), with *Chiropodomys* recovered as sister to the Hydromyine (Lecompte *et al.*, 2008; Rowe *et al.*, 2008), and *Vandeleuria* was resolved as closely related to the tribes Apodemurini + Praomyini (Rowe *et al.*, 2008). Within the Rattini (clade A), we recovered four main monophyletic lineages: (1) the Southeast Asian genus *Maxomys* and the Philippine–Sulawesi genus *Crunomys* (clade C); (2) the *Melasmothrix* lineage; (3) the *Dacnomys* division clade (clade E); and (4) the *Rattus* division clade (clade F), as recovered in previous analyses (Steppan *et al.*, 2005; Jansa *et al.*, 2006; Lecompte *et al.*, 2008; Rowe *et al.*, 2008; Pagès *et al.*, 2010; Balakirev, Abramov & Rozhnov, 2011; Balakirev *et al.*, 2012).

All three markers (cyt*b*, *GHR*, and *IRBP*) strongly supported the inclusion of *Halmaheramys* within the *Rattus* clade (more precisely, clade H; Fig. 2). This clade consisted of four major groups: (1) the Sri Lankan endemic *Srilankamys*; (2) the Southeast Asian *Berylmys*; (3) the Indo-Pacific clade containing the Sulawesian *Bunomys*, *Paruromys*, and *Taeromys*, Moluccan *Halmaheramys*, Philippine *Bullimus*, and Sundaic *Sundamys* (clade H); and (4) a clade containing the Southeast Asian *Rattus* (clade M), Philippine rats (*Rattus everetti*, *Tarsomys*, and *Limnomys*; clade N), the South/Southeast Asian *Nesokia* + *Bandicota* (clade L), and the Japanese *Diplothrix* and Sahul *Rattus* (clade K). The well-supported node H revealed a simultaneous split among *Halmaheramys*, *Sundamys* + *Bullimus*, and the Sulawesian clade (clade I) containing *Bunomys*, *Paruromys*, and *Taeromys*. Within this Sulawesian clade (clade I), we recovered the monophyletic *Paruromys* and *Taeromys* as sister to *Bunomys*; however, our current gene and taxon sampling were unable to resolve the phylogenetic relationships amongst this larger cluster (Fig. 2). Despite this lack of resolution, our results indicated that *Halmaheramys* is nested within this western Indo-Pacific clade (clade H). The proposed western origin of this species is the first example in which a native murine endemic to Halmahera may have arrived immediately in the Moluccas from the western Indo-Pacific (other Moluccan native rodents, classified in the genera *Rattus*, *Nesoromys*, *Melomys*, *Uromys*, and *Hydromys* show phylogenetic links, demonstrated or speculated, to relatives that occur in

the Australo-Papuan region; Flannery, 1995; Helgen, 2003).

In this study, we have provided the first molecular phylogenetic evidence for the relationships of *R. morotaiensis*, which we found to be closely related to the Sahul *Rattus* clade (clade K; Taylor *et al*., 1982; Robins *et al*., 2010; Rowe *et al*., 2011). Another native Halmaheran endemic, an undescribed species of *Melomys* (Fabre *et al*., 2013), was also found to be closely related to the Australo-Papuan lineages (the *M. burtoni*/*M. lutillus* group). Our results indicated a close relationship between several Sundaic, Sulawesian, and Philippine lineages with the Moluccan *Halmaheramys*. The island of Halmahera appears unique within the Moluccas so far (also see the Discussion), in that it includes two native lineages of Rattini with independent colonization routes: one originating from a western ancestor, likely to be associated with Sulawesi (*Halmaheramys*), and one from an eastern ancestor, likely to be associated with Sahul (*R. morotaiensis*).

Our concatenated mitochondrial and nuclear data set allowed us to provide new insights regarding the systematics of the Rattini, and refined and revised existing phylogenetic hypotheses from previous treatments (Musser, 1981; Musser & Newcomb, 1983; Musser & Holden, 1991; Musser & Carleton, 2005; Steppan *et al*., 2005; Jansa *et al*., 2006; Lecompte *et al*., 2008; Rowe *et al*., 2008; Balakirev *et al*., 2012). However, resolution of the evolutionary affinities among genera in the *Rattus* division (clade F), specifically among the different *Rattus* lineages from the Philippines, Southern Asia, Southeast Asia, and Sahul, remains incomplete, and will remain so until additional molecular data, particularly representing additional taxa, become available (as in Rowe *et al*., 2011; Pagès *et al*., 2013). Based on previous results (Jansa *et al*., 2006; Lecompte *et al*., 2008; Rowe *et al*., 2008; Pagès *et al*., 2010) and those presented in this study, we propose the definition of seven new *Rattus* lineages: (1) a monospecific *Srilankamys* lineage; (2) a monogeneric *Berylmys* lineage; (3) an unnamed Indo-Pacific lineage comprising *Bullimus*, *Bunomys, Paruromys*, *Halmaheramys*, *Sundamys*, and *Taeromys*; (4) an unnamed lineage containing the Southeast Asian and Sundaic species of *Rattus* and the Sulawesian *R. hoffmanni*; (5) an unnamed lineage comprising the Philippine taxa *Rattus everetti*, *Tarsomys*, and *Limnomys*; (6) an unamed lineage comprising *Bandicota* and *Nesokia*; and (7) an unamed lineage containing the Japanese *Diplothrix* and all Sahul endemic *Rattus*. Future studies should aim at improving resolution throughout the Rattini phylogeny by: (1) increasing taxon sampling (and thus reducing the number of isolated branches); (2) increasing the sampling of DNA characters through the addition of

further mitochondrial and nuclear markers; and/or (3) searching for loci that contain rare genomic changes (e.g. indels and retroposons); and (4) searching for new morphological characters to supplement phylogenetic results, including the use of new morphometric geometric and taxonomic tools.

IMPLICATIONS FOR THE BIOGEOGRAPHY OF INDO-PACIFIC MURINAE

Our biogeographical analyses were unable to resolve the ancestral area of the Murinae. This uncertainty most likely reflects the simultaneous colonization and explosive diversification by murines across the landmasses of Asia (Rattini), Africa (Arvicanthini, Praomyini, Otomyini), and the Philippines (Phloeomyini). The Philippines appear to have been a key area for the early radiation of the Murinae, with many basal lineages within the group (Phloeomyini and Hydromyini); however, our ancestral reconstructions also indicated a prominent role for South/Southeastern Asia as a source pool for murine taxa that subsequently colonized Africa, the Indo-Pacific islands, and the Palaearctic. Regarding Indo-Pacific Rattini (Figs 3, 4), our biogeographical analysis indicated that colonizations occurred mainly from mainland Asia and the Sunda Shelf, with at least one re-colonization from Sahul to Wallacea (*R. morotaiensis*, Halmahera).

Our phylogenetic results indicated three key colonization periods: (1) arrival in the Philippines (Phloeomyini) during the Late Miocene (Tortonian); (2) dispersal of both Sahul/Philippine Hydromyini and Sulawesi/Philippine Rattini during the late Miocene; and (3) multiple Plio-Pleistocene colonizations of the Rattini into the Indo-Pacific area (at least six events). Changing sea levels during the Plio-Pleistocene have been suggested to have influenced the colonization events of many organisms across Indo-Pacific insular contexts (Mercer & Roth, 2003; Hall, 2009). This may have been particularly important in the shallow parts of the Indo-Pacific archipelagos, where islands currently separated by sea were connected during periods of lowered sea level (Voris, 2000). Our results seem to indicate a strong influence of these eustatic sea level variations on the distribution of the Murinae, with no inferred colonizations occurring during the period of high sea level in the early Pliocene (Zanclean; Fig. 4), then followed by several colonizations in the subsequent periods of low sea levels.

The Indo-Pacific islands of the Philippines, Sahul, and Sulawesi host three main lineages of Murinae. These lineages differ not only in their timing of origin but also their routes of colonization (Figs 3, 4). During the Plio-Pleistocene, the Rattini (clade A), originating

from Southeast Asia, rapidly colonized Wallacea, the Philippines, and the remote Sahul Shelf. During this period, these areas underwent repeated sea level fluctuations, which have been suggested to explain similar patterns of dispersal identified for numerous organismal groups within this region, such as marsupials (Macqueen, Goldizen & Seddon, 2009), reptiles (Williams *et al.*, 2009), and rodents (Mercer & Roth, 2003; Rowe *et al.*, 2008, 2011; Bryant *et al.*, 2011). One possible explanation for the differences in distribution and apparent colonization patterns among the Murinae lineages could be that the Rattini simply represent the most recently successful clade within the Southeast Asian region, diversifying explosively since the Late Miocene, and possibly displacing older Indo-Pacific murine lineages (Phloeomyini and Hydromyini). Consequently, these older Indo-Pacific murine representatives may be relicts of an earlier radiation that was historically more widespread across the Indo-Pacific (Jansa *et al.*, 2006; Rowe *et al.*, 2008). Past extinctions of crown Phloeomyini and Hydromyini may obscure substantially earlier biogeographical distributions of these lineages in the Indo-Pacific. In summary, dispersal and extinction no doubt play an important role in the distribution and structure of murine assemblages, but much remains to be learned about the pattern and timing of murine rodents across the complex geography of the Indo-Pacific region.

SULAWESI AND HALMAHERA DIVERSIFICATION OF THE MURINAE

In contrast to the Philippine archipelago, where at least three murine tribes are found, Sulawesi appears to have been colonized relatively recently by murine rodents (Fig. 4). This conclusion is based upon generic-level phylogenetic analyses of the DNA sequences currently available. However, several Sulawesi endemic Rattini and *Micromys* division genera are lacking in published DNA databases, and their inclusion in future studies is needed to further test our conclusions. As for most of the Sulawesi fauna (Sarasin & Sarasin, 1901; Wallace, 1910; Stresemann, 1939; Whitmore, 1987; Whitten, Mustafa & Henderson, 2002), the murine biota is considered to be of Asian origin. We inferred that most of the dispersals from Southeast Asia/Sundaland that generated the Sulawesian murine fauna occurred between the late Miocene and the Plio-Pleistocene. These findings agree with molecular phylogenetic reconstructions for various animal groups of Sulawesi (Stelbrink *et al.*, 2012), including herpetofauna (Evans *et al.*, 2003a, b, 2008), mammals (Evans *et al.*, 1999, 2003b, c; Mercer & Roth, 2003; Alfaro *et al.*, 2008; Esselstyn, Timm & Brown, 2009; Merker

et al., 2009), and arthopods (Butlin *et al.*, 1998). The relatively recent colonization of Sulawesi has been linked to: (1) the increase of Sulawesian landmass availability caused by the collision of the Sula spur with both the northern and western arms of Sulawesi (Hall *et al.*, 1988; Hall, 2002, 2009); and (ii) the periodic sea level lowstand that started during the Mid-Miocene, with highstands during the Late Miocene and Plio-Pleistocene.

Our analyses revealed that at least two main lineages of Rattini have undergone independent diversifications in Sulawesi, with the shrew-like *Melasmothrix* lineage and another radiation comprising at least two scansorial rats (*Taeromys* and *Paruromys*). Further sampling is required to clarify the systematics and biogeographical history of the Rattini and the role that Sulawesi has played in their evolution. The addition of further shrew-rat genera (from the *Echiothrix*, *Melasmothrix*, *Maxomys*, and *Crunomys* divisions) will be particularly important for future work. This last genus (*Crunomys*) displays complex distributional patterns involving both Sulawesi and the Philippines, possibly indicative of a historical connection and potential routes of colonization between these regions (for further discussion, see Evans *et al.*, 2003a).

With respect to the Moluccas (Ambon, Banda, Buru, Seram, Halmahera, Kai, Obi, Sula, Talaud, and Tanimbar groups, and their associated smaller islands), only two genera of Rattini are known, one of which is endemic to Seram (*Nesoromys*), whereas the other is widespread [*Rattus*, containing *Rattus elaphinus* (Sody, 1941), *R. morotaiensis*, and *Rattus feliceus* (Thomas, 1920)]. Whereas species diversity in the Rattini is substantial in Sulawesi (Musser & Holden, 1991; Musser & Durden, 2002; Musser & Carleton, 2005), this is not the case on other Wallacean islands, where Hydromyini seems to be the better represented lineage (Helgen, 2003). The Moluccas harbours a murine fauna that mainly originates from the eastern part of the Indo-Pacific (Sahul–New Guinea and Australia). Because of its location and geological history, the island of Halmahera supports a fauna that mostly displays clear Sahul origins, with a few endemic taxa coming from the western Indo-Pacific, especially in mammals. Our phylogenetic study indicates that the ancestors of *Halmaheramys* most likely colonized Halmahera from the west (probably from Sulawesi) during the Pliocene (Figs 2, 3). At least two other Halmaheran taxa (*R. morotaiensis* and an undescribed species of *Melomys*) colonized the North Moluccas later, probably in the Pleistocene, but from the east (Sahul). Thus, Halmahera constitutes a unique transition zone in the Moluccas for the murines, colonized from both the east and the west. This pattern, a Wallacean hallmark, is shared

with Sulawesi, famous for being a remarkable zone of biotic overlap for non-volant mammals, where western components of Asian origin (murines, squirrels, ungulates, civets, etc.) and eastern components of Sahulian origin (endemic phalangers) co-occur. The route of colonization from the west is surprising given that Halmahera is thought to have always been separated from Sulawesi, and is currently surrounded by strong sea currents (the Halmahera Eddy and associated current; Arruda & Nof, 2003). This pattern of colonization may be linked with two geological/climatological events: (1) the beginning of climatically induced sea-level lowstands in the Late Pliocene (Haq, Hardenbol & Vail, 1987; De Graciansky *et al*., 1998), and (2) the advent of contact between two volcanic arcs *c*. 3 Mya (Hall, 2002, 2009). The geological and biogeographical history of Halmahera is closely linked to that of the Australo-Papuan region (Hall *et al*., 1988; Hall, 2009), with several biogeographical studies demonstrating a close link between these faunas (*e.g.* de Jong, 1998; Helgen, 2003). Before the complete formation of New Guinea, Halmahera had already begun to rift east from its current position along the Pacific plate, starting in the early Miocene (Hall *et al*., 1988, Hall & Nichols, 1990; Hall, 2002; 2009), and is currently closer to Sulawesi than during most of its history. During the Mid Miocene, the Halmahera and Sangihe arcs collided for the first time, creating a unique, double subduction system. This Moluccan Sea subduction zone may have generated past terrestrial connections, better facilitating the arrival of Rattini (and other colonizers) from the west Indo-Pacific areas to the North Moluccas. Whatever the precise route of colonization, the immediate origins of Halmahera's Rattini, involving colonizations from both east and west, point to the importance of complex patterns of dispersal (and back dispersal) in assembling the murine fauna of the Moluccas. The Moluccas remain one of the least explored regions of the Indo-Pacific region for mammal biodiversity. As with *Halmaheramys* gen. nov., we suggest that the discovery of many additional native rodents in the region will clarify the biogeographical origins and subsequent evolution of myriad unique rodent faunas on the many biotically obscure oceanic island constellations that populate the very heart of the Malay Archipelago, bounded to the north, south, east, and west, respectively, by the rich murine faunas of the Philippines, Australia, New Guinea, and Sulawesi.

IMPLICATION FOR THE MURINAE FOSSIL CONSTRAINTS

The node ages inferred among the three calibration settings (see Material and methods, Results, and Table 2) differed by less than 5%. Apart from the Hydromyini calibration, the Apodemurini, the *Apodemus*/*Sylvaemus*, the *Mus*, and the Arvicanthini divergences included their median palaeontological ages, and the confidence intervals for the molecular date estimates are contained within all the fossil dates (see Table 2). This result is reassuring with respect to the ability of Bayesian methods to handle rate heterogeneity and multiple fossil constraints in the Murinae lineages. Considering the time intervals, the aforementioned fossil constraints can be considered as cross-validated: 75% of the molecular confidence intervals were contained within the palaeontological interval. We used the upper and the lower bounds around the *Progonomys*/*Antemus* fossil calibration and the 95% confidence interval of the Bayesian dating estimates to distribute these two calibration settings into four categories: (1) the molecular interval is included in the palaeontological interval; (2) the palaeontological interval is included in the molecular interval; (3) the two intervals overlap; and (4) the two intervals are separate. The Phloeomyini/core Murinae and core Murinae split settings both belong to category 3 (Table 2). Both aforementioned fossil constraints can be considered as cross-validated, but respectively 94% of the molecular confidence intervals of the Phloeomyini/core Murinae divergence were contained within the palaeontological interval [11.8 Mya (10.4–13.7 Mya) for the molecular data versus 12.1 Mya (10.01–22.9 Mya) for the fossil data], whereas only 34% of the molecular confidence intervals of the core Murinae were contained within the palaeontological interval [10.3 Mya (9.2–11.6 Mya) for the molecular data versus 12.1 Mya (10.01–22.9 Mya) for the fossil data]. Consequently, our cross-validation analysis of the *Antemus*/*Progonomys* calibration followed the assignment of Steppan *et al*. (2004), who argued that this fossil must be placed on the Phloeomyini/core Murinae divergence, and not on the core Murinae divergence. These results suggest a palaeontological versus molecular discrepancy. This observation would indicate that the placement of the *Antemus*/*Progonomys* found within the Siwalik formation (Middle Miocene, Pakistan; Jacobs & Pilbeam, 1980; Jacobs *et al*., 1990; Jacobs & Downs, 1994) is uncertain, and justifies a placement at the root of the Murinae. Therefore, the divergence of extant core Murinae seems to be more recent than the palaeontological boundaries defined by Jacobs & Downs (1994). This suggests that the corresponding fossils might be linked to extinct stem lineages without direct relation to crown core Murinae. Alternatively, there is the possibility that extensive substitution rate variations have occurred along the Murinae branch, leading to difficulties in the dating estimation under the relaxed molecular clock model. In view of these cross-validation results, we choose to

REFERENCES

Aguilar J-P, Michaux J. 1996. The beginning of the age of Murinae (Mammalia: Rodentia) in southern France. *Acta Zoologica Cracoviensia* **39:** 35–45.

Alfaro ME, Karns DR, Voris HK, Brock CD, Stuart BL. 2008. Phylogeny, evolutionary history, and biogeography of Oriental-Australian rear-fanged water snakes (Colubroidea: Homalopsidae) in-ferred from mitochondrial and nuclear DNA sequences. *Molecular Phylogenetics and Evolution* **46:** 576–593.

Aplin KP. 2006. Ten million years of rodent evolution in Australasia: phylogenetic evidence and a speculative historical biogeography. In: Merrick JR, Archer M, Hickey GM, Lee MSY, eds. *Evolution and biogeography of Australasian vertebrates*. Sydney: Auscipub Pty Ltd, 707–744.

Aplin KP, Helgen KM. 2010. Quaternary murid rodents of Timor. Part I: new material of *Coryphomys buehleri* Schaub, 1937, and description of a second species of the genus. *Bulletin of the American Museum of Natural History* **341:** 1–80.

Arruda WZ, Nof D. 2003. The Mindanao and Halmahera eddies–twin eddies by nonlinearities. *American Meteorological Society* **33:** 2815–2830.

Balakirev AE, Abramov AV, Rozhnov VV. 2011. Taxonomic revision of *Niviventer* (Rodentia, Muridae) from Vietnam: a morphological and molecular approach. *Russian Journal of Theriology* **10:** 1–26.

Balakirev AE, Abramov AV, Tikhonov AN, Rozhnov VV. 2012. Molecular phylogeny of the *Dacnomys* Division (Rodentia, Muridae): the taxonomic positions of *Saxatilomys* and *Leopoldamys*. *Doklady Biological Sciences* **445:** 251–254.

Balakirev AE, Rozhnov VV. 2010. Phylogenic relationships and species composition in the genus *Niviventer* (Rodentia, Muridae) based on studies of the cytochrome b gene of mtDNA. *Moscow University Biological Sciences Bulletin* **65:** 170–173.

Balete DS, Rickart EA, Heaney LR, Alviola PA, Duya MV, Duya MRM, Sosa T, Jansa SA. 2012. *Archboldomys* (Muridae, Murinae) reconsidered : a new genus and three new species of shrew mice from Luzon Island, Philippines. *American Museum Novitates* **3754:** 1–60.

Benton MJ, Donoghue PC, Asher RJ. 2009. Calibrating and constraining the molecular clock. In: Hedges B, Kumar S, eds. *Dating the tree of life*. Oxford: Oxford University Press, 35–86.

Benton MJ, Donoghue PCJ. 2007. Paleontological evidence to date the Tree of Life. *Molecular Biology and Evolution* **24:** 26–53.

Bryant LM, Donnellan SC, Hurwood DA, Fuller SJ. 2011. Phylogenetic relationships and divergence date estimates among Australo-Papuan mosaic-tailed rats from the *Uromys* Division (Rodentia: Muridae). *Zoologica Scripta* **40:** 433–447.

Butlin RK, Walton C, Monk KA, Bridle JR, Hall R, Holloway JD. 1998. Biogeography of Sulawesi grasshoppers, genus *Chitaura*, using DNA sequence data. In: Hall R, Holloway JD, eds. *Biogeography and geological evolution of SE Asia*. Leiden: Backhuys Publishers, 355–359.

Buzan EV, Pagès M, Michaux J, Krystufek B. 2011. Phylogenetic position of the Ohiya rat (*Srilankamys ohiensis*) based on mitochondrial and nuclear gene sequence analysis. *Zoologica Scripta* **40:** 545–553.

Carleton MD. 1980. Phylogenetic relationships in Neotomine-Peromyscine rodents (Muroidea) and a reappraisal of the dichotomy within New World Cricetinae. *Miscellaneous Publications Museum of Zoology, University of Michigan* **157:** 1–146.

Carleton MD, Musser GG. 1984. Muroid rodents. In: Anderson S, Jones JK, Jr, eds. *Orders and families of recent mammals of the world*. New York: Wiley, 289–379.

Carleton MD, Musser GG. 1989. Systematic studies of oryzomyine rodents (Muridae, Sigmodontinae): a synopsis of *Microryzomys*. *Bulletin of the American Museum of Natural History* **191:** 1–83.

De Graciansky P-C, Hardenbol J, Jacquin T, Vail PR. 1998. Mesozoic and Cenozoic sequence stratigraphy of European basins. *The Society of Economic Paleontologists and Mineralogists* Special Publication 60.

Douzery EJP. 2011. Molecular phylogeny: inferring the patterns of evolution. In: Gargaud M, Lopez-Garcia P, Martin H, eds. *Origins and evolution of life: an astrobiological perspective*. Cambridge: Cambridge University Press, 291–312.

Drummond AJ, Nicholls GK, Rodrigo AG, Solomon W. 2002. Estimating mutation parameters, population history and genealogy simultaneously from temporally spaced sequence data. *Genetics* **161:** 1307–1320.

Drummond AJ, Rambaut A. 2007. BEAST: bayesian evolutionary analysis by sampling trees. *BMC Evolutionary Biology* **7:** 214.

Edwards ID, Payton RW, Proctor JP, Riswan S. 1990. Altitudinal zonation of the rain forests in Manusela National Park, Seram, Maluku, Indonesia. In: Baas P, Kalkman K, Geesink R, eds. *The plant diversity of Malesia. Proceedings of the Flora Malesiana Symposium commemorating Professor Dr. C.G.G.J. van Steenis*. Leiden: Kluwer Academic Publishers, 161–175.

Ellerman JR. 1941. *The families and genera of living rodents. vol II. Family Muridae*. London: British Museum (Natural History).

Ellerman JR. 1949. *The families and genera of living rodents. vol. III*. London: British Museum (Natural History).

Esselstyn JA, Achmadi AS, Rowe KC. 2012. Evolutionary novelty in a rat with no molars. *Biology Letters* **8:** 990–993.

Esselstyn JA, Timm RM, Brown RM. 2009. Do geological or climatic processes drive speciation in dynamic archipelagos? The tempo and mode of diversification in Southeast Asian shrews. *Evolution* **63:** 2595–2610.

Evans BJ, Brown RM, McGuire JA, Supriatna J, Andayani N, Diesmos A, Iskandar D, Melnick DJ, Cannatella DC. 2003a. Phylogenetics of fanged frogs: testing biogeographical hypotheses at the interface of the Asian and Australian faunal zones. *Systematic Biology* **52:** 794–819.

Evans BJ, McGuire JA, Brown RM, Andayani N, Supriatna J. 2008. A coalescent framework for comparing alternative models of population structure with genetic data: evolution of Celebes toads. *Biology Letters* **4:** 430–433.

Evans BJ, Morales JC, Supriatna J, Melnick DJ. 1999. Origin of the Sulawesi macaques (Cercopithecidae, *Macaca*) as inferred from a mitochondrial DNA phylogeny. *Biological Journal of the Linnean Society* **66:** 539–560.

Evans BJ, Supriatna J, Andayani N, Melnick DJ. 2003c. Diversification of Sulawesi macaque monkeys: decoupled evolution of mitochondrial and autosomal DNA. *Evolution* **57:** 1931–1946.

Evans BJ, Supriatna J, Andayani N, Setiadi MI, Cannatella DC, Melnick DJ. 2003b. Monkeys and toads define areas of endemism on Sulawesi. *Evolution* **57:** 1436–1443.

Fabre P-H, Fitriana YS, Pagès M, Jønsson KA, Michaux J, Semiadi G, Supriatna N, Helgen KM. 2013. A new species of *Melomys* (Mammalia Rodentia, Murinae) from Halmahera (North Moluccas, Indonesia). *Zookeys*.

Felsenstein J. 1985. Confidence limits on phylogenies: an approach using the bootstrap. *Evolution* **39:** 783–791.

Flannery TF. 1995. *Mammals of the south-west Pacific & Moluccan Islands*. Chatswood, NSW: Reed Books.

Hall R. 1996. Reconstructing Cenozoic SE Asia. In: Hall R, Blundell DJ, eds. *Tectonic Evolution of SE Asia, Vol. 106*. London: Geological Society of London Special Publication, 153–184.

Hall R. 2002. Cenozoic geological and plate tectonic evolution of SE Asia and the SW Pacific: computer-based reconstructions, model and animations. *Journal of Asian Earth Sciences* **20:** 353–434.

Hall R. 2009. Indonesia, geology. In: Gillespie R, Clague D, eds. *Encyclopedia of islands*. Berkeley, CA: University of California Press, 454–460.

Hall R, Audley-Charles MG, Banner FT, Hidayat S, Tobing S. 1988. Late Palaeogene–Quaternary geology of Halmahera, Eastern Indonesia: initiation of a volcanic island arc. *Journal of the Geological Society* **145:** 577–590.

Hall R, Cottam M, Wilson MEJ. 2011. *The SE Asian Gateway: history and tectonics of Australia-Asia collision*. London: Geological Society of London (Special Publication).

Hall R, Nichols G. 1990. Terrane amalgamation in the Philippine sea margin. *Tectonophysics* **181:** 207–222.

Haq BU, Hardenbol J, Vail P. 1987. Chronology offluctuating sea levels since the Triassic. *Science* **235:** 1156–1167.

Heaney LR, Balete DS, Dolar ML, Alcala AC, Dans ATL, Gonzales PC, Ingle NR, Lepiten MV, Oliver WLR, Ong PS, Rickart EA, Tabaranza JBR, Utzurrum RCB. 1998. A synopsis of the mammalian fauna of the Philippine Islands. *Fieldiana Zoology New Series* **88:** 1–61.

Heaney LR, Balete DS, Rickart EA, Veluz MJ, Jansa SA. 2009. A new genus and species of small 'tree mouse' (Rodentia, Muridae) related to the Philippine giant cloud-rats. *Bulletin of the American Museum of Natural History* **331:** 205–229.

Helgen KM. 2003. A review of the rodent fauna of Seram, Moluccas, with the description of a new subspecies of mosaic-tailed rat, *Melomys rufescens paveli*. *Journal of Zoology* **261:** 165–172.

Ho SYW, Kolokotronis S-O, Allaby RG. 2007. Elevated substitution rates estimated from ancient DNA sequences. *Biology Letters* **3:** 702–705.

Irwin DM, Kocher TD, Wilson AC. 1991. Evolution of the cytochrome *b* gene of mammals. *Journal Molecular Evolution* **32:** 128–144.

Jacobs LL, Downs WR. 1994. The evolution of murine rodents in Asia. In: Tomida Y, Li C, Setoguchi T, eds. *Rodent and lagomorph families of Asian origins and diversification*. Tokyo: National Science Museum, Tokyo, Monograph Series.149–156.

Jacobs LL, Flynn JJ. 2005. Of mice . . . again: the Siwalik rodent record, murine distribution, and molecular clocks. In: Leiberman DE, Smith RJ, Kelley J, eds. *Interpreting the past: essays on human, primate, and mammal evolution in honor of David Pilbeam*. Boston, MA: Brill Academic Publishers Inc, 63–80.

Jacobs LL, Flynn LJ, Downs WR, Barry JC. 1990. Quo Vadis Antemus? The Siwalik muroid record. In: Lindsay EH, Fahlbusch V, Mein P, eds. *European neogene mammal chronology NATO ASI ser. A: life sciences*. New York: Plenum Press, 573–586.

Jacobs LL, Pilbeam D. 1980. Of mice and men: fossil-based divergence dates and molecular 'clocks. *Journal of Human Evolution* **9:** 551–555.

Jaeger JJ, Tong H, Denys C. 1986. The age of the *Mus-Rattus* divergence – Paleontological data compared with the molecular clock. *Comptes Rendus de l'Academie des Sciences, Serie II* **302:** 917–922.

Jansa SA, Barker FK, Heaney LR. 2006. The pattern and timing of diversification of Philippine endemic rodents: evidence from mitochondrial and nuclear gene sequences. *Systematic Biology* **55:** 73–88.

Jansa SA, Giarla TC, Lim B. 2009. The phylogenetic position of the rodent genus *Typhlomys* and the geographic origin of Muroidea. *Journal of Mammalogy* **90:** 1083–1094.

Jansa SA, Weksler M. 2004. Phylogeny of muroid rodents: relationships within and among major lineages as determined by IRBP gene sequences. *Molecular Phylogenetics and Evolution* **31:** 256–276.

de Jong R. 1998. Halmahera and Seram: different histories, but similar butterfly faunas. In: Hall R, Holloway JD, eds. *Biogeography and geological evolution of SE Asia*. Leiden: Backhuys Publishers, 315–325.

Katoh K, Toh H. 2010. Parallelization of the MAFFT multiple sequence alignment program. *Bioinformatics* **26:** 1899–1900.

Kellogg R. 1945. Two rats from Morotai Island. *Proceedings of the Biological Society of Washington* **58:** 65–68.

Lartillot N, Lepage T, Blanquart S. 2009. PhyloBayes 3: a Bayesian software package for phylogenetic reconstruction and molecular dating. *Bioinformatics* **25:** 2286–2288.

Lartillot N, Philippe H. 2004. A Bayesian mixture model for across-site heterogeneities in the amino-acid replacement process. *Molecular Biology and Evolution* **21:** 1095–1109.

Lartillot N, Philippe H. 2009. Improvement of molecular phylogenetic inference and the phylogeny of Bilateria. In: Telford MJ, Littlewood DTJ, eds. *Animal evolution: genomes, fossils, and trees*. Oxford: Oxford University Press, 127–138.

Lecompte E, Aplin K, Denys C, Catzeflis F, Chades M, Chevret P. 2008. Phylogeny and biogeography of African Murinae based on mitochondrial and nuclear gene sequences, with a new tribal classification of the subfamily. *BMC Evolutionary Biology* **8:** 199.

Lemmon AR, Brown JM, Strager-Hall K, Lemmon EM. 2009. The effect of ambiguous data on phylogenetic estimates obtained by maximum likelihood and Bayesian inference. *Systematic Biology* **58:** 130–145.

Lohman DJ, de Bruyn M, Page T, von Rintelen K, Hall R, Ng PKL, Shih H-T, Carvalho GR, von Rintelen T. 2011. Biogeography of the Indo-Australian Archipelago. *Annual Review of Ecology, Evolution, and Systematics* **42:** 205–226.

Lundrigan BL, Jansa SA, Tucker PK. 2002. Phylogenetic relationships in the genus *Mus*, based on paternally, maternally, and biparentally inherited characters. *Systematic Biology* **51:** 410–431.

Macqueen P, Goldizen A, Seddon J. 2009. Response of a southern temperate marsupial, the Tasmanian pademelon (*Thylogale billardierii*), to historical and contemporary forest fragmentation. *Molecular Ecology* **18:** 3291–3306.

Martin Suarez E, Mein P. 1998. Revision of the genera *Parapodemus*, *Apodemus*, *Rhagamys* and *Rhagapodemus* (Rodentia, Mammalia). *Geobios* **31:** 87–97.

Medway L, Yong H-S. 1976. Problems in the systematics of the rats (Muridae) of Peninsular Malaysia. *Malaysian Journal of Science* **4:** 1–4.

Mercer JM, Roth VL. 2003. The effects of Cenozoic global change on squirrel phylogeny. *Science* **299:** 1568–1572.

Merker S, Driller C, Perwitasari-Farajallah D, Pamungkas J, Zischler H. 2009. Elucidating geological and biological processes underlying the diversification of Sulawesi tarsiers. *Proceedings of the National Academy of Sciences of the United States of America* **106:** 8459–8464.

Michaux J, Aguilar J-P, Legendre S, Montuire S, Wolf A. 1997. Les Murinae (Rodentia, Mammalia) néogènes du sud

de la France: evolution et paléoenvironnements. *Geobios* **20:** 379–385.

Michaux J, Reyes A, Catzeflis F. 2001. Evolutionary history of the most speciose mammals: molecular phylogeny of muroid rodents. *Molecular Biology and Evolution* **18:** 2017–2031.

Misonne X. 1969. African and Indo-Australian Muridae: evolutionary trends. *Musée Royal de l'Afrique Centrale Tervuren Belgique Annales Sciences Zoologiques* **172:** 1–219.

Monk KA, Fretes Y, Reksodiharjo-Lilley G. 1997. *The ecology of Nusa Tenggara and Malulu. The Ecology of Indonesia Series Vol. V*. Hong Kong: Periplus Editions Ltd.

Musser GG. 1981. The giant rat of Flores and its relatives east of Borneo and Bali. *Bulletin of the American Museum of Natural History* **169:** 67–176.

Musser GG. 1987. The mammals of Sulawesi. In: Whitmore TC, ed. *Biogeographic evolution of the Malay Archipelago*. Oxford: Oxford University Press, 73–93.

Musser GG. 1991. Sulawesi rodents: descriptions of new species of *Bunomys* and *Maxomys* (Muridae, Murinae). *American Museum Novitates* **3001:** 1–41.

Musser GG, Carleton MD. 2005. Order Rodentia. In: Wilson ED, Reeder DM, eds. *Mammal species of the world: a taxonomic and geographic reference Vol. 2, 3rd edn*. Baltimore: Johns Hopkins University Press. 895–1531.

Musser GG, Durden LA. 2002. Sulawesi rodents: description or a new genus and species of murinae (Muridae, Rodentia) and its parasitic new species of sucking louse (Insecta, Anoplura). *American Museum Novitates* **3368:** 1–50.

Musser GG, Heaney LR. 1992. Philippine rodents: definitions of *Tarsomys* and *Limnomys* plus a preliminary assessment of phylogenetic patterns among native Philippine murines (Murinae, Muridae). *Bulletin of the American Musum of Natural History* **211:** 1–138.

Musser GG, Holden ME. 1991. Sulawesi rodents (Muridae, Murinae) – morphological and geographical boundaries of species in the *Rattus-Hoffmanni* group and a new species from Pulau-Peleng. *Bulletin of the American Museum of Natural History* **206:** 322–413.

Musser GG, Lunde DP. 2009. Systematic review of New Guinea *Coccymys* and '*Melomys*' *albidens* (Muridae, Murinae) with descriptions of new taxa. *Bulletin of the American Museum of Natural History* **329:** 1–139.

Musser GG, Newcomb C. 1983. Malaysian murids and the giant rat of Sumatra. *Bulletin of the American Museum of Natural History* **174:** 327–598.

Pagès M, Bazin E, Galan M, Chaval Y, Claude J, Herbreteau V, Michaux J, Piry S, Morand S, Cosson JF. 2013. Cytonuclear discordance among Southeast Asian black rats (*Rattus rattus* complex). *Molecular Ecology* **2:** 1019–1034.

Pagès M, Chaval Y, Herbreteau V, Waengsothorn S, Cosson J-F, Hugot J-P, Morand S, Michaux J. 2010. Revisiting the taxonomy of the Rattini tribe: a phylogeny-based delimitation of species boundaries. *BMC Evolutionary Biology* **10:** 184.

Parham JF, Donoghue PCJ, Bell CJ, Calway DT, Head JJ, Holroyd PA, Inoue JG, Irmis RB, Joyce WA, Ksepka DT, Patané JSL, Smith ND, Tarver JE, van Tuinen M, Yang Z, Angielczyk KD, Greenwood J, Nipsley CA, Jacobs L, Makovicky PJ, Müller J, Smith KT, Theodor JM, Warnock RCM, Benton MJ. 2012. Best practices for applying paleontological data to molecular divergence dating. *Systematic Biology* **61:** 346–359.

Philippe H. 1993. MUST: a computer package of management utilities for sequences and trees. *Nucleic Acids Research* **21:** 5264–5272.

Philippe H, Brinkmann H, Lavrov DV, Littlewood DT, Manuel M, Wörheide G, Baurain D. 2011. Resolving difficult phylogenetic questions: why more sequences are not enough. *PLoS Biology* **9:** e1000602.

Posada D. 2008. jModelTest: phylogenetic model averaging. *Molecular Biology and Evolution* **25:** 1253–1256.

Posada D, Crandall KA. 1998. ModelTest: testing the model of DNA substitution. *Bioinformatics* **14:** 817–818.

Poux C, Douzery EJ. 2004. Primate phylogeny, evolutionary rate variations, and divergence times: a contribution from the nuclear gene IRBP. *American Journal of Physical Anthropology* **124:** 1–16.

Rambaut A, Drummond AJ. 2007. Tracer v1.4, Available at: http://beast.bio.ed.ac.uk/Tracer

Ree RH, Moore BR, Webb CO, Donoghue MJ. 2005. A likelihood framework for inferring the evolution of geographic range on phylogenetic trees. *Evolution* **59:** 2299–2311.

Ree RH, Smith SA. 2008. Maximum likelihood inference of geographic range evolution by dispersal, local extinction, and cladogenesis. *Systematic Biology* **57:** 4–14.

Rickart EA, Heaney LR, Goodman SM, Jansa S. 2005. Review of the Philippine genera *Chrotomys* and *Celaenomys* (Muridae) and description of a new species. *Journal of Mammalogy* **86:** 415–428.

Rickart EA, Heaney LR, Tabaranza Jr BR. 2002. Review of *Bullimus* (Muridae: Murinae) and description of a new species from Camiguin Island, Philippines. *Journal of Mammalogy* **83:** 421–436.

Robins JH, Hingston M, Matisoo-Smith E, Ross HA. 2007. Identifying *Rattus* species using mitochondrial DNA. *Molecular Ecology ressources* **7:** 717–729.

Robins JH, McLenachan PA, Phillips MJ, McComish BJ, Matisoo-Smith E, Ross HA. 2010. Evolutionary relationships and divergence times among the native rats of Australia. *BMC Evolutionary Biology* **10:** 375.

Ronquist F, Huelsenbeck JP. 2003. MrBayes 3: bayesian phylogenetic inference under mixed models. *Bioinformatics* **19:** 1572–1574.

Rowe KC, Aplin KP, Baverstock PR, Moritz C. 2011. Recent and rapid speciation with limited morphological disparity in the genus *Rattus*. *Systematic Biology* **60:** 188–203.

Rowe KC, Reno ML, Richmond DM, Adkins RM, Steppan SJ. 2008. Pliocene colonization and adaptive radiations in Australia and New Guinea (Sahul): multilocus systematics of the old endemic rodents (Muroidea : Murinae). *Molecular Phylogenetics and Evolution* **47:** 84–101.

Sarasin P, Sarasin F. 1901. *Ueber die geologische Geschichte der Insel Celebes auf Grund der Thierverbreitung*. Wiesbaden: Kreidel.

Sidiyasa K, Tantra IGM. 1984. Analisis flora pohon hutan dataran rendah Wae Mual, Taman Nasional, Seram-Maluku. *Bulletin Penlitian Hutan (Forest Research Bulletin)* **462:** 19–34.

Stamatakis A. 2006. RAxML-VI-HPC: maximum likelihood-based phylogenetic analyses with thousands of taxa and mixed models. *Bioinformatics* **22:** 2688–2690.

Stelbrink B, Albrecht C, Hall R, von Rintelen T. 2012. The biogeography of Sulawesi revisited: is there evidence for a vicariant origin of taxa on Wallace's 'anomalous island'? *Evolution* **66:** 2252–2271.

Steppan SJ, Adkins RM, Anderson J. 2004. Phylogeny and divergence-date estimates of rapid radiations in muroid rodents based on multiple nuclear genes. *Systematic Biology* **53:** 533–553.

Steppan SJ, Adkins RM, Spinks PQ, Hale C. 2005. Multigene phylogeny of the Old World mice, Murinae, reveals distinct geographic lineages and the declining utility of mitochondrial genes compared to nuclear genes. *Molecular Phylogenetics and Evolution* **37:** 370–388.

Stresemann E. 1939. Die Vögel von Celebes. *Journal of Ornithology* **87:** 299–425.

Swofford DL. 2002. PAUP*. Phylogenetic Analysis Using Parsimony(and Other Methods), 4: Sunderland, MA.

Taylor JM, Calaby JH, Van Deusen HM. 1982. A revision of the genus *Rattus* (Rodentia, Muridae) in the New Guinean region. *Bulletin of the American Museum of Natural History* **173:** 177–336.

Taylor JM, Horner BE. 1973. Results of the Archbold Expeditions. No. 98. Systematics of native Australian *Rattus* (Rodentia: Muridae). *Bulletin of the American Museum of Natural History* **150:** 1–130.

Tedford RH, Wells RT, Barghoorn SF. 1992. Tirari formation and contained faunas, Pliocene of Lake Eyre Basin, South Australia. *Beagle (Records of the Northern Territory Museum of Arts and Sciences)* **9:** 173–194.

Vangegeim EA, Lungu AN, Tesakov AS. 2006. Age of Vallesian lower boundary (continental Miocene of Europe). *Stratigraphy and Geological Correlation* **14:** 655–667.

Voris HK. 2000. Maps of Pleistocene sea levels in Southeast Asia: shorelines, river systems and time durations. *Journal of Biogeography* **27:** 1153–1167.

Voss RS. 1988. Systematics and ecology of ichthyomyine rodents (Muroidea): patterns of morphological evolution in a small adaptive radiation. *Bulletin of the American Museum of Natural History* **188:** 259–493.

Wallace AR. 1910. *The world of life*. London: Chapman.

Whitmore TC. 1987. *Biogeographical evolution of the Malay Archipelago*. Oxford: Clarendon Press.

Whitten AJ, Mustafa M, Henderson GS. 2002. *The ecology of Sulawesi*. Singapore: Periplus.

Williams M, Cook E, van der Kaars S, Barrows T, Shulmeister J, Kershaw P. 2009. Glacial and deglacial climatic patterns in Australia and surrounding regions from 35 000 to 10 000 years ago reconstructed from terrestrial and near-shore proxy data. *Quaternary Science Reviews* **28:** 2398–2419.

Winkler AJ. 2002. Neogene paleobiogeography and East African paleoenvironments: contributions from the Tugen Hills rodents and lagomorphs. *Journal of Human Evolution* **42:** 237–256.

Xia X, Lemey P. 2009. Assessing substitution saturation with DAMBE. In: Lemey P, Salemi M, Vandamme AM, eds. *The phylogenetic handbook: a practical approach to DNA and protein phylogeny*. Cambridge: Cambridge University Press, 615–630.

Xia X, Xie Z. 2001. DAMBE: data analysis in molecular biology and evolution. *Journal of Heredity* **92:** 371–373.

Xia X, Xie Z, Salemi M, Chen L, Wang Y. 2003. An index of substitution saturation and its application. *Molecular Phylogenetics and Evolution* **26:** 1–7.

APPENDIX

Collecting localities of *Halmaheramys bokimekot* gen. et sp. nov. and *Rattus morotaiensis* species in Halmahera, Indonesia.

HALMAHERAMYS

***Halmaheramys bokimekot* gen. et sp. nov.** – Central Halmahera Boki mekot area: MZB 33261–266

RATTUS

Rattus morotaiensis – Central Halmahera Tofu Blewen MZB 33228, MZB 33231, MZB 33244, MZB 33258, Central Halmahera North Ake Jira: MZB 33469.

Voucher studied in this study.

Measurements derived from the following specimens of *Bunomys*, *Taeromys*, and *Paruromys* were used for the principal component analyses.

BUNOMYS

Bunomys chrysocomus – Bogani Nani Wartabone National Park: AMNH 256885–889; LAD 18; SAM 12617, 12621, 12627, 12629. Bumbarujaba: USNM 218127, 218128, 218132–135, 218140 (holotype of *nigellus*). Sungai Oha Kecil + Sungai Sadaunta: AMNH 224054, 224078, 224079, 224081–086, 224088–091, 224093, 224095, 224096, 224099–105, 224109–114, 224118–126, 224128–135, 224137–140, 224143, 224647, 224649–660, 224662–671, 224673–688, 224692–694, 224696–703, 224706, 224709, 224711, 224713–715, 224717, 224719–725, 224728, 224729, 224731, 224733–747, 224750, 224752, 224755–758, 224762–765, 224767–769, and 227730. Danau Lindu Valley + Gunung Kanino: AMNH 223040, 223044, 223050–053, 223055, 223057, 223059, 223062, 223064, 223065, 223069, 223078, 223079, 223081, 223082, 223292, 223297–223300, 223302, 223303, 223308, 223310, 223312, 223314, 223317, 223319, 223468, 223567, 223568, 224154–224156, 225148;

USNM 218691, 218692, 218702, 218704. Gimpu: USNM 219580, 219595 (holotype of *rallus*), 219713. Bakubakulu: AMNH 229519. Gunung Balease: MVZ 225697, 225714, 225810. Gunung Tambusisi: AMNH 265077, 265078; MZB 12181, 12183, 12185; SAM 15588. Pegunungan Mekongga: AMNH 101195, 101197, 101200, 101202, 101211, 101217, 101220, 101223, 101224, 101234, 101236 (holotype of *koka*). Lalolei: AMNH 101052, 101055 (holotype of *lalolis*), 101288.

Bunomys coelestis – Gunung Lompobatang: AMNH 101132, 101133, 101135, 101137, 101138, 101141–101144, 101149, 101150, 101152, 101153, 101155, 101157, 101158; BMNH 97.1.3.12 (holotype of *coelestis*).

Bunomys prolatus – Gunung Tambusisi: AMNH 265074–076; MZB 12187, 12188, 12190 (holotype of *prolatus*), 12191, 12193.

Bunomys fratrorum – Teteamoet: USNM 216836, 216837, 216839, 216841, 216843, 216887–889, 216892, 216894, 216895, 216897, 216899, 216902–904, 216906, 216907, 216909–915, 216919, 216920, 216922–926. Kuala Prang: USNM 217587, 217589–591, 217594, 217596–600, 217602, 217603, 217605, 217606, 217609, 217611, 217613, 217614, 217827–829, 217831, 217832, 217834, 217835, 217837. Gunung Klabat: USNM 217581, 217585. Rurukan: BMNH 97.1.2.28 (holotype of *fratrorum*). Temboan: USNM 217624, 217635, 217638, 217639, 217643, 217648–651, 217653, 217655, 217656, 217659, 217661, 217662, 217666, 217668, 217670, 217854, 217856–858, 217866, 217868, 217869, 217876, 217880, 217881, 217887, 217896, 217898, 217900, 217902 Gunung Maujat + Gunung Mogogonipa: SAM 12616, 12619, 12623, 12644.

B. andrewsi – Pulau Buton: AMNH 31294; USNM 175899 (holotype of *andrewsi*). Labuan Sore: USNM 218115, 218138. Kuala Navusu + Pinedapa: AMNH 225647–649, 225651–658, 225661–663; USNM 219581, 219587, 219589, 219591, 219593, 219594, 219596, 219600, 219601, 219602 (holotype of *adspersus*), 219603, 219605, 219606, 219619, 219620, 219622. Sungai Ranu: AMNH 249942–945; CHSW 36. Sukamaju: AMNH 229720. Gunung Balease: MVZ 225683, 225685, 225688, 225689, 225695, 225708, 225710, 225812. Desa Lawaki Jaya: MVZ 225691, 225698, 225699, 225702, 225719–721. Wawo + Masembo: AMNH 101059 (holotype of *inferior*), 101061, 101069, 101072. Puro-Sungai Miu: AMNH 257187, 257189, 224630–633, 224107, 224116. Tamalanti: BMNH 40.446–40.448, 40.450–40.452. Tuare: USNM 219598, 219599. Mamasa area: AMNH 267796–798, 267800–804, 267806, 267807; MZB 34912, 34913, 34916, 34917, 34926, 34955. Lombasang: AMNH 100996–100998, 101004, 101006 (holotype of *heinrichi*), 101009, 101010.

Bunomys penitus – Gunung Kanino: AMNH 223805, 223806, 223809, 223811, 223814, 223815, 223819–822, 223826, 223828, 223829, 223831–833, 223835, 223836, 223829, 223840, 223842, 223845–850, 223852, 223904–907, 225251, 225253, 225254, 225256, 225257, 225260, 225262, 225264, 225265, 225267, 225269, 225271–273, 225275, 225276, 225278–285, 225287, 225288, 225290–293, 225295–302, 225304–306, 225376. Gunung Nokilalaki: AMNH 223853, 223855, 223857, 223859, 223861–866, 223868, 223870–875, 223878–882, 223885–888, 223892, 223895–897, 223899–902, 225307, 225308, 225310–315, 225317–325, 225328–333, 225335, 225336, 225338, 225340–342, 225344–346, 225348–354, 225359, 225361–365, 225368, 225369. Rano Rano: USNM 219627 (holotype of *sericatus*), 219630, 219631. Gunung Lehio: USNM 218682–684, 218686 (holotype of *penitus*), 218687. Mamasa area: AMNH 267790, 267793, 267794; MZB 34845, 34848–50. Pegunungan Latimojong: AMNH 196587, 196588, 196590. Pegunungan Mekongga: AMNH 101193, 101196, 101209, 101210, 101213, 101216, 101222, 101227, 101231, 101235, 101237.

TAEROMYS

Taeromys celebensis – Teteamoet: USNM 216795, 216801, 216806. Mapangat: RMNH 2821. Kuala Prang: USNM 217673, 217675–678. Amurang: RMNH 2801. Temboan: RMNH 21052, 21053; USNM 217683, 217695, 217698. Tolitoli: USNM 200261, 200264. Sungai Oha Kecil: AMNH 224539, 224640. Sungai Miu: AMNH 224071, 224072, 224074, 224075. Sungai Sadaunta: AMNH 224069, 224070, 224641, 224643–645. Tomado: AMNH 223027, 223029, 223031, 223032, 223283, 223284, 223565, 224076, 224077. Sungai Tokararu: AMNH 223285, 223287. Kuala Navusu: AMNH 225671–673. Sungai Tolewonu: AMNH 226411–413. Pinedapa: USNM 219562, 219565, 219706, 219707. Wawo: AMNH 101044, 101075, 101076.

Taeromys callitrichus – Rurukan: BMNH 97.1.2.26 (holotype of *maculipilis*), 97.1.2.27. 'Northeastern Arm': RMNH 21255. Sungai Sadaunta: AMNH 224637, 224638. Gunung Kanino: AMNH 225125. Gunung Nokilalaki: AMNH 225126. Kulawi: BMNH 40.388 (holotype of *jentinki*). Tamalanti: BMNH 40.389.

Taeromys microbullatus – Pegunungan Mekongga: AMNH 101108 (holotype of *microbullatus*), 101109.

Taeromys arcuatus – Pegunungan Mekongga: AMNH 101107, 101110, 101111 (holotype of *arcuatus*), 101113–115; MZB 5813.

Taeromys taerae – Rurukan: AMNH 101244. Lembean: RMNH 22569 (holotype of *taerae*), 22570, 22571, 36388.

Taeromys hamatus – Gunung Kanino: AMNH 223369, 223461, 223701, 223700. Gunung Nokilalaki:

AMNH 223702, 223703, 223705, 225149, 225151, 225152. Gunung Lehio: USNM 218680 (holotype of *hamatus*), 218685.

Taeromys punicans – Pinedapa: USNM 219625 (holotype of *punicans*).

PARUROMYS

Northern peninsula – Teteamoet: USNM 216797, 216802–804, 216807–812, 216814, 216815, 216993. Kuala Prang: USNM 217674, 217679, 217680. Rurukan: AMNH 101252. Gunung Masarang: BMNH 97.1.2.24 (holotype of *dominator*). Temboan: USNM 217681, 217682, 217684–687, 217689, 217690, 217693, 217696, 217697, 217700, 217903. Ile-Ile: AMNH 101280. Sungai Paleleh: USNM 200253, 200255, 200258. Tolitoli: USNM 200262, 200265.

Core – Kuala Navusu: AMNH 225687–689, 225691, 225692, 225694, 225696, 225698–701, 225703–709, 225711–715, 225717–719, 225721–725, 225728–732, 225735, 225736, 225742–745, 225747, 225749, 225751–753, 225939. Sungai Tolewonu: AMNH 226415–418, 226420–423, 226425–433, 226435, 226436. Pinedapa: USNM 219548, 219557, 219564, 219566 (holotype of *camurus*), 219728. Sungai Oha

Kecil: AMNH 224805. Sungai Miu; AMNH 224174, 224176–178, 224180. Sungai Sadaunta: AMNH 224173, 224808, 224810, 224811, 224813, 224815, 224816, 224818–820, 224822, 224824, 224826–832, 224834, 224835, 224839, 224840, 224844. Sungai Tokararu + Gunung Kanino: AMNH 223332, 223334, 223336, 223338, 223340, 223342, 223348, 223351, 223352, 223355, 223573, 223575–577, 223583, 223584, 233588, 223646, 223647, 223649, 225380–382, 225384–395, 225397–402, 225404, 225453–455. Gunung Nokilalaki: AMNH 203606, 223596, 223597, 223600, 223605, 223609, 223613, 223621, 223626, 223629, 223632, 223635–637, 223642, 223643, 223645, 225406–416, 225418, 225422–427, 225430–432, 225434–436, 225438, 225441–446. Lambanan + Sumarorong: AMNH 267746, 267750–754.

Southeastern Peninsula – Wawo + Pegunungan Mekongga: AMNH 101077, 101116–118, 101120, 101122, 101176.

Southwestern Peninsula – Gunung Lompobatang: AMNH 101123, 101160, 101162, 101164–167, 101171–174; MZB 5593 (holotype of *ursinus*).

SUPPORTING INFORMATION

Additional supporting information may be found in the online version of this article at the publisher's web-site:

Table S1. Taxonomic sampling, voucher numbers, and loci used in this study.